Kinetic study and modelling of drying of *Chlorella vulgaris*
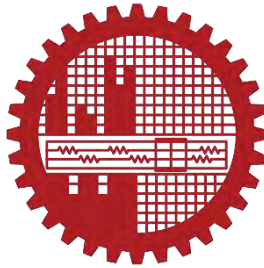
by

Debabrata Karmakar

MASTER OF SCIENCE IN CHEMICAL ENGINEERING

Department of Chemical Engineering

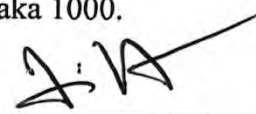BANGLADESH UNIVERSITY OF ENGINEERING AND TECHNOLOGY

February, 2021

The thesis titled "Kinetic study and modelling of drying of *Chlorella vulgaris*" Submitted by Debabrata Karmakar, Roll No: 1015022033, Session: October, 2015 has been accepted as satisfactory in partial fulfilment of the requirement for the degree of Master of Science in Chemical Engineering on 27 February, 2021.

BOARD OF EXAMINERS

1. Dr. Kazi Bayzid Kabir   Chairman
   Associate Professor
   Department of Chemical Engineering
   BUET, Dhaka 1000.

2. Dr. Md. Mominur Rahman   Member
   Professor and Head   (Ex-Officio)
   Department of Chemical Engineering
   BUET, Dhaka 1000.

3. Dr. Ijaz Hossain   Member
   Professor
   Department of Chemical Engineering
   BUET, Dhaka 1000.

4. Dr. Kawnish Kirtania   Member
   Assistant Professor
   Department of Chemical Engineering
   BUET, Dhaka 1000.

5. Dr. Mohammad Ismail   Member
   Associate Professor   (External)
   Department of Applied Chemistry and Chemical Engg
   University of Dhaka, Dhaka-1000.

CANDIDATES DECLARATION

It is hereby declared that this thesis or any part of it has not been submitted elsewhere for the award of any degree or diploma.

(Debabrata Karmakar)

ACKNOWLEDGEMENT

All the praise to Almighty, who has made all the attempts and efforts fruitful.

I would like to thank all the great people who contributed in some way to the work described in this thesis.

First of all, I would also like to thank my thesis supervisor **Dr. Kazi Bayzid Kabir**. The door to his office was always open whenever I ran into a trouble spot or had a question about my research or writing. He consistently allowed this paper to be my own work, but steered me in the right the direction whenever he thought I needed it.

I am also grateful to the following university staff: Mr. John Biswas, Md. Ismail Hossain for their unfailing support and assistance.

Finally, I must express my very profound gratitude to my parents and to my brother for providing me with unfailing support and continuous encouragement throughout my years of study and through the process of researching and writing this thesis. This accomplishment would not have been possible without them. Thank you.

ABSTRACT

Microalgae are an incredibly diverse group of eukaryotic organisms that thrive in a wide range of habitats. Microalgae not only have a significant potential as a supplement of fossil fuels but also as a source of a wide spectrum of chemicals, including PUFAs (Polyunsaturated fatty acids), carotenoids, and antioxidants. They are the most efficient biomass producer compared to others. But there is a great challenge to use this microorganism efficiently. Microalgae grow in aqueous media (Growth media, Waste water etc.). To use it in bio-fuel production, producing different chemical extraction or making nutraceutical product for human or animal consumption, it has to be dried first. Extensive studies have been done on the benefits and uses of microalgae, but very few are focusing drying. In this study, one species of microalgae (*Chlorella vulgaris*) was studied for determining the drying kinetics in the moisture removal process. Drying behavior data was obtained from TGA (Thermogravimetric analysis) and DSC (Differential scanning calorimetry). The moisture content of biomass decreased rapidly with increase in temperature and an approximate peak was obtained in the temperature range of 65-80^{0}C. Four non-isothermal drying models were obtained from four popular drying kinetics model generally used for studying drying kinetics of agricultural products. These models were evaluated based on the coefficient of determination (R^2) and reduced chi-square (χ^2). Page's model was found to be the best fitted model for describing the drying kinetics.

TABLE OF CONTENTS

LIST OF FIGURES

LIST OF TABLES

LIST OF SYMBOLS AND ABBREVIATION

a	Empirical model constant (dimensionless)
a_1, a_2	Geometric constants
AR	Aspect ratio (dimensionless)
ASTM	American Standard Test Method
b	Empirical model constant (dimensionless)
BCSIR	Bangladesh Council of Scientific and Industrial Research
BUET	Bangladesh University of Engineering and Technology
c	Empirical model constant (dimensionless)
CARS	Centre for Advanced Research in Sciences
d	Empirical constant (K^{-1})
DB	Dry Basis
DHA	Docosahexaenoic Acid
DM	Dry Matter
DSC	Differential scanning calorimetry
DTG	Differential Thermo Gravimetry
e	Empirical constant (dimensionless)
E_a	Activation energy for diffusion (kJ/mol) or (W/g)
EPA	Eicosapentaenoic Acid
FFA	Free fatty Acid
g	Drying constant obtained from experimental
h	Drying constant obtained from experimental
H	Humidity (g water / kg dry air)
i	Number of terms of the infinite series
I	Radiation intensity (W/cm^2)
k, k_1, k_2	Drying constants obtained from experimental
k_0	Pre-exponential constant (s^{-1})
k_{th}	Theoretical value of drying constant (s^{-1})
M	Local moisture content (kg water/kg dry matter)
Me	Equilibrium moisture content (% dry basis)
M_i	Initial moisture content (% dry basis)
M_t	Mean moisture content at time t (% dry basis)

MBE	Mean Bias Error
MCD	Millicandela
MPE	Mean Percent Error
MR	Moisture Ratio
MSE	Mean Square Error
N	Number of observations
n	Empirical model constant (dimensionless);
OD	Optical Density
P	Pressure (kPa)
PUFA	Polyunsaturated fatty acid
RMSE	Root Mean Square Error
SSE	Sum square error
TG	Thermogravimetry
TGA	Thermogravimetric analysis
UTEX	University of Texas
WB	Wet Basis

1. INTRODUCTION

1.1 Background

"Algae" is a colloquial term and refers to a large group of photosynthetic eukaryotes. It can grow almost anywhere and hence plays an important role in the ecosystem. They participate in the bio-remediation process by removing heavy metals from water bodies, as a feedstock in health-supplements, animal feeds, bio-char, bio-sorbents, or for the production of bio-energy [1]. Algal biomass offers a number of advantages over conventional biomass due to high productivity, use of non-productive land, recovery of waste-nutrients, effective sequestration of greenhouse gas, etc. [2].

In recent years, microalgae are being preferred over macroalgae because of their higher growth rate, higher yield and higher lipid content etc. [3]. Among the varieties of microalgae, *Chlorella vulgaris*, which can be easily cultured, display the best suitability toward large scale oil production [4].

Generally, freshly harvested microalgae contain more than 80%-90% of moisture, which needs to be reduced to about 10% for any useful application [5]. The moisture content needs to be reduced to approximately 10% to maximize oil extraction from algae [6]. Therefore, drying is the most important part for making a viable product from microalgae.

The knowledge of drying kinetics is necessary to describe the combined macroscopic and microscopic mechanisms of mass transfer during the drying processes [7]. The drying kinetics models are essential for effective design, accurate simulation and efficient optimization of the drying processes. For engineering applications, models that are simple and have reasonable interpretation of the physical phenomena must be selected. Alongside the material characteristics, the knowledge of the drying kinetics of the material is also essential for proper designing of dryers.

There are several existing kinetic models for biomass drying e.g., Newton, Logarithmic, Page, Midilli etc. [8, 9]. These models have been developed during the drying of various food and agricultural products [10-13]. However, very few studies are available to understand the drying kinetics of microalgae.

1.2 Objectives

The overall objective of this research work is to find a suitable kinetic model that can be applicable for the drying of *Chlorella vulgaris*. This will help in identifying optimized

and cost-effective drying conditions. To achieve this, the proposed work has some specific objectives which include

➢ The identification of mass loss pattern during the non-isothermal drying of *Chlorella vulgaris*
➢ Finding out the most suitable drying kinetics model using existing models
➢ The development of a new model, if necessary.

1.3   Scope

Huge varieties of microalgae species are available over the world. There exists fresh water species as well as saline water species. Among this diverse group of species in this present study, *Chlorella vulgaris* has been studied for determining the kinetics of the moisture removal process. This species is a freshwater variant and easy to cultivate. They grow in normal freshwater without special requirement of conditions and it contains notable amount of lipid too for bio-fuel production. Moreover, this species had been preserved and cultivated at BCSIR laboratories. So, availability of pure species locally also makes the study limited to it. There are also a number of *Chlorella vulgaris* strain available, only the strain available at BCSIR strain has been considered here. The target of this work is to study the drying kinetics. Drying means the removal of moisture and there are three types of moisture available in a material in general. To study the drying behavior of moisture removal, Thermogravimetric analysis (TGA); and to learn about the presence of different types of moisture, Differential scanning calorimetry (DSC) test have been done. And the most suitable kinetics model has been evaluated by evaluating the experimental data. Due to the complexity involved, in this study four simple semi-theoretical models were studied to match with the drying kinetic of *Chlorella vulgaris*.

1.4   Methodology

In order to meet all the requirements of the expected objectives, the research work of this thesis has been divided into three sub-sections.

1.4.1   Characterization

As a first step, the characterization of the sample has been done. The organic elemental composition (C, H, N, S, O) of microalgae species (*Chlorella vulgaris*) has been achieved by CHNS/O analysis while physical composition (moisture, volatiles, fixed carbon, ashes etc.) has been evaluated by proximate analysis. Heating value has also been obtained by bomb calorimeter experiment.

1.4.2 Mass loss pattern observation

Mass loss pattern of the sample has been observed by Thermogravimetric analysis (TGA) during non-isothermal drying at two different heating rates (5ºK/min and 20 ºK /min), operating from room temperature to 600ºC. The amount of heat required to increase the temperature during drying process has been measured by Differential scanning calorimetry (DSC), operating from room temperature to 300 ºC.

1.4.3 Modelling

TGA data obtained from one heating rate has been used to fit the existing kinetic models for biomass drying. Four popular kinetic models namely Newton, Logarithmic, Henderson and Pabis and Page have been used here. The goodness of fit criteria (coefficient of determination (R^2) and reduced chi-square ($\chi2$)) has been used to determine the best fit. The parameters obtained from the best fitted model have been used to predict the drying behavior for the other heating rate.

1.5 Thesis organization

Chapter 1 introduces the overall summery of the thesis work. The importance of the field of research and its impacts on environment, on our daily life have been discussed in short. Moreover, objectives, all possible outcomes have been mentioned along with the methodology.

Chapter 2 is the literature review section. It focuses on *Chlorella vulgaris,* the type of microalgae we are interested to. Various uses of it were discussed. The classification of *Chlorella vulgaris* was discussed along with its bio-chemical compositions. In later part of this section, drying mechanism was explained and various methods were illustrated along with kinetics models. At the end the necessity of drying kinetics and importance of research in this topic were discussed.

Materials and Methods were discussed in Chapter 3. This section contains the way which have been followed to perform the objectives of this thesis work in details.

Chapter 4 is the result and discussion section. All the results obtained during the thesis work have been discussed here. Significance of the findings were also mentioned in this section.

Chapter 5 is for conclusion and future recommendations. Some recommendations were made in which field the research work can be continued in future.

2. LITERATURE REVIEW

2.1 Introduction

Microalgae are the fastest growing microscopic photosynthetic organisms, since their cell doubling time can be as little as a few hours [14]. Microalgae can grow both in marine and freshwater environments. Microalgae can convert solar energy, CO_2 and nutrients to biomass efficiently, which can be further processed into bio-fuel, food and various important compounds. The ability of microalgae to fix CO_2 from the environment is around 10 times more than any kind of terrestrial plants. They also use solar energy and consume the harmful pollutants from the environment, while not competing with food crops [15].

Because of the presence of different valuable compounds, microalgae are being cultivated for various bio-chemicals generally used in human food, aquaculture and pharmaceutical industries. Microalgae find uses in aquaculture industry for the production of live feed like Daphnia, Moina etc., for juvenile stages of fish and for zooplankton used in aquaculture food chains.

Table 2.1 shows the comparative data for various plant generally used for bio-fuel production along with their productivity and land use.

Table 2.1 :Comparison of microalgae with other bio-diesel feedstock [16]

Plant source	Seed oil content (% oil by wt in biomass)	Oil yield (L oil/ ha-year)	Land use (m2 year/kg bio-diesel)	Bio-diesel productivity (kg bio-diesel /ha year)
Corn/Maize (*Zea mays L.*)	44	172	66	152
Hemp (*Cannabis sativa L.*)	33	363	31	321
Soybean (*Glycine max L.*)	18	636	18	562
Jatropha (*Jatropha curcas L.*)	28	741	15	656
Camelina (*Camelina sativa L.*)	42	915	12	809
Sunflower (*Helianthus annuus L.*)	40	1070	11	946

Castor (*Ricinus communis*)	48	1307	9	1156
Palm oil (*Elaeis guineensis*)	36	5366	2	4747
Microalgae (low oil content)	30	58,700	0.2	51,927
Microalgae (medium oil content)	50	97,800	0.1	86,515
Microalgae (high oil content)	70	136,900	0.1	121,104

From Table 2.1 the relative benefits of microalgae compared to other plant for bio-fuel production can easily be understood. Currently a lot of plants are being used for bio-fuel production. Some of them are from our food list and makes scarcity of food to some level and also requires a huge number of lands. But microalgae are above these problems. Microalgae with high oil content can produce around 800 times more oil compared to corn/maize in a specific amount of land. Although microalgae represent an extensive biodiversity worldwide, the bulk amount of biomass is can be represented by four strain only. These are: Cyanobacterium (*Spirulina)* and Green microalgae *(Chlorella*, *Dunaliella* and *Haematococcus)* [14]. Among them *Chlorella vulgaris* is the most remarkable green eukaryotic microalgae, classification of which has been given in Table 2.2.

Table 2.2: Classification of *Chlorella vulgaris*

Domain	Eukaryota
Kingdom	Protista
Division	Chlorophyta
Class	Trebouxiophyceae
Order	Chlorellales
Family	Chlorellaceae
Genus	*Chlorella*
Species	*Chlorella vulgaris*

Chlorella Vulgaris is found worldwide, since it is so adaptable to its environment. This variety has high temperature tolerance capacity, since some strains can grow between 15 and 40 ^{0} C.

The general bio-chemical composition of *C. vulgaris* is shown in the Table 2.3. The main component is the protein which represents more than 50% of the chemical composition of *C. vulgaris* biomass.

Table 2.3: Bio-chemical composition of *Chlorella vulgaris* (dry matter basis). [17]

Component	%
Crude Protein	51-58
Carbohydrates	12-17
Lipid	14-22
Nucleic acid	4-5

Biochemical composition of *Chlorella vulgaris* varies a lot from culture to culture. It varies with growth medium, pH, light, temperature, growth stage etc. It has been found that the variation at different growth stage is mainly due to nutrient depletion, particularly if an organism is grown in batch culture.

The protein content in some microalgae species can be high and hence they can be considered as an unconventional source of protein. Protein content in *C. Vulgaris* can be as high as 58%, higher than dried skimmed milk, soy flour and chicken [18].

Chlorella cultivation is popular around the world because of its use as a food and feed supplement, also as a potential source of raw materials for pharmaceutical and cosmetics industries. Also, Chlorella can synthesize a significant amount of storage compounds like polysaccharides or neutral lipids. This happens usually under high irradiance with nutrient deficiency. From Table 2.3 it can also be seen that under optimal growth conditions around 14–22% lipids per dry weight of biomass can be reached. These lipids include hydrocarbons, phospholipids and some free fatty acids. If the product is bio-diesel feedstock, the cell is stressed to produce the maximal amount of lipid. During such unfavorable growth conditions, lipids content (mainly composed of triacylglycerol) can reach up to 58% [19].

Carbohydrates is one of the major components of the analysis of *Chlorella vulgaris* as can be seen in Table 2.3. Starch, sugars, glucose and some other polysaccharides can be found present in Chlorella as carbohydrates. Among which starch is the most abundant one [19]. *Chlorella* is also rich in pigments like chlorophyll, carotenoids etc. *Chlorella* is also a promising source of minerals including Ca, K, Mg and Zn [20] along with nearly all essential vitamins (e.g., A, B_1, B_2, B_6, B_{12}, C, E, nicotinate, biotin, folic acid and pantothenic acid).

2.2 Mechanism of Drying

Drying is the process of the removal of water or other liquids from any substances. The mechanisms of drying usually includes: surface diffusion from the pore surfaces, capillary action and diffusion due to differences in moisture [21]. While mass is transferred from the solid to the surroundings in the form of water vapor, heat is transferred from the surrounding to the product. The rate of drying depends on both these phenomena of heat and mass transfer.

Usually, for hygroscopic materials the drying process starts at constant rate and subsequent falling rate period. The drying stops when the moisture content reaches the equilibrium amount.

The surface film of the materials appears to be dried after sometimes of starting of the process. After reaching the critical moisture content, the first falling rate appears. The falling rate period is mainly controlled by liquid diffusion. Moisture diffusion happens due to the concentration differences and depends on internal conditions like moisture content, temperature and the structure of the materials. After sometime, the first falling rate period gets replaced by the second falling rate periods. Vapor diffusion is the driving force of this period which is due to moisture concentration difference and some internal conditions of the materials.
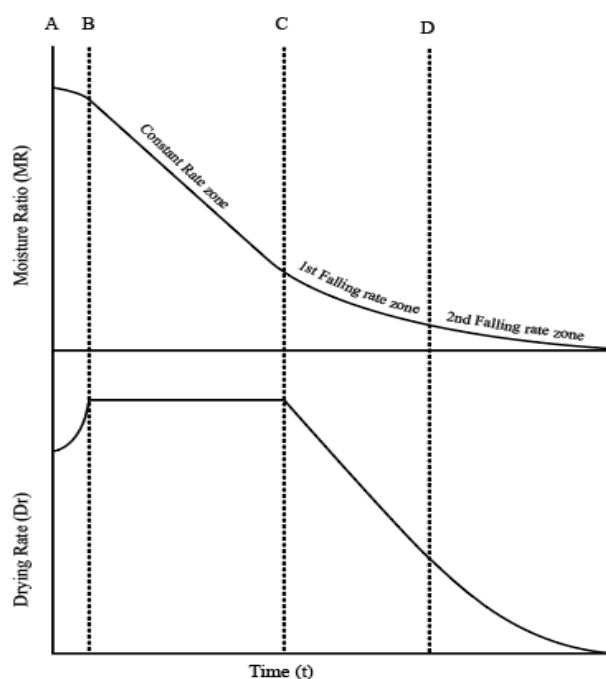
Figure 2-1: Different stages of drying process

Figure 2-2 [22] shows the relation of the drying rate and moisture ratio with time. In initial drying period, the ambient air temperature remains greater than the temperature of the product. This causes an increase in the drying rate (between lines A and B) as well as an increase in the product's temperature until it reaches line B. During the constant rate period the evaporation takes place at the surface of the wet solid after which the falling rate period comes. The falling rate period can be divided into two different steps: (i) first falling rate period and (ii) second falling rate period. The first falling rate period (C to D in Figure 2-3) starts when the surface film of the material becomes dry, and the moisture content has decreased to its critical moisture content. In the first falling rate period, a decrease in the wetted surface causes decrease in the rate of drying. After some time, the drying step will change from the first falling rate period to the second falling rate period (D to E), where internal liquid diffusion controls the drying process.

2.3   Drying methods of *Chlorella vulgaris*

After harvesting microalgae, usually a dewatering process is carried out, which reduces the moisture to some extent but not enough. Further moisture removal is necessary through different drying process. Drying brings the moisture to a lower level and minimizes the deterioration and spoilage due to microbial activities. Drying also minimizes transportation, storage, packaging cost and time.

There are several drying processes which can be employed: solar drying, convective drying, spray drying, freeze drying, etc. The choice of methods depends on the requirement of the final products and the sanitary level required [23].

2.3.1   Solar drying

Solar drying is the cheapest methods of all available processes. But this process requires a large drying surface with a long drying time. It is also not possible to maintain the quality of the final product and the rate of drying is very slow. Longer time gives chance of rising total bacterial count. For this reason, closed solar devices are usually used. However, temperature in such devices may vary between 35^0 C and 60^0 C, making it hard to control the product quality [24].

2.3.2   . Convective drying

Convective drying is another form of popular drying method in case of effectiveness after solar drying. Usually, the oil yield of dried biomass in both convective and solar methods are the same. But the efficiency of the convective method is better than the solar drying

method. The free fatty acids (FFAs) content is the same as obtained with freeze drying [24].

2.3.3 Spray drying

There is another process of drying which can produce a dark green powder of dried microalgae. It is mainly used to produce high value microalgal products. The color and nutrient content of the final product greatly depend on the drying process and temperature. If it is compared with the convective drying process, it can be found that the biomass dried in spray dryer will retain more nutrient content, while 20-30% loss in proteins will occur in case of convective drying [24].

2.3.4 Freeze drying

Freeze drying is another type of drying method commonly used in food industries. It is also very popular for research purpose as all the cells are preserved without rupturing the cell wall in this method. Among the processes mentioned so far, freeze drying keeps the highest amount of proteins in the dried biomass.

2.3.5 Other drying technologies

There are some other drying processes available in the literature. Roller/drum drying is one of them. It is mostly used in food industry. In case of microalgae drying both drying and disruption of cell can be achieved simultaneously. Another type of drying process is fluidized-bed drying system. It is commonly used to dry different grains and fruits. The efficiency of heat and mass transfer is very remarkable. It also requires short drying time, and the quality of products are also very high.

2.4 Drying Kinetics

Drying processes mainly involve physical and chemical (biochemical) reaction. These changes occur at a specific rate along with specific kinetics. The kinetic modeling of the process parameters plays an important role to understand and predict the behavior of drying clearly. The changes and the rates can be expressed quantitatively by using kinetic equation. Kinetic modeling can also identify the dominant mechanisms involved in the drying process.

To identify the most suitable drying method and to have control over the drying process knowledge of drying kinetics is a must. To use the drying process for engineering calculation or to optimize the process it will also be required. Full-scale experimentation

to determine the most suitable operating conditions for drying of certain material is costly and time consuming. Drying kinetic makes it possible to express the process by equations and the relation to the process variables. So, a good understanding of the drying rate is important for developing appropriate drying model.

2.4.1 Thin Layer Drying Process

Drying process almost always has a temperature gradient between the air and the temperature of the material to be dried. There is also a temperature gradient along the depth of the solid mass. But by reducing thickness of the materials can easily minimize these gradients to an acceptable value [25]. Thin layer is nothing but a layer of materials with sufficiently thin thickness so that air characteristics remain uniform everywhere in the layer without variance. Thin layer drying process also refers the drying of materials fully exposed to the drying air.

Generally, drying process can be divided into two periods. They are the constant drying rate period and the falling drying rate period. During constant rate period, the solid material contains high moisture and hence the surface somehow behaves like a liquid surface. It is similar as the drying of an open-faced body of water. The water present in the material and the conditions of the environment will determine the rate of drying. In this period solid do not have any role on drying rate. Some of the common materials which dries initially under this period are wet sand, soil, washed seeds etc. Conduction, convection, or radiation provides energy required during this step.

But in practice, for most solids, especially agricultural products, most of the drying takes place during the falling rate period. This period is bounded by equilibrium moisture content of the material. This falling rate period can be further subdivided into two process named first falling rate and second falling rate period.

2.4.2 Theory of Drying Kinetics Studies for Thin Layer

Drying includes both mass and energy transfer simultaneously. It describes the effect of different process variables on moisture. It also gives an idea about the mechanism of moisture removal process. The actual mechanism is very hard to understand and also the process of finding it is complex [26].

A number of researchers have developed computer models to predict the moisture content of biomass samples as a function of temperature using thin layer drying phenomena [27]. Thin layer drying kinetics equations give the idea about the physical mechanism that take

place during the drying process, in a less complicated and less time-consuming way. Instead of very complex data in theoretical models, this simple and easy to understand models have been used in studying and describing various agricultural products drying process. In thin layer modelling it is considered that the product thickness is sufficiently small to consider that the air characteristics is identical and uniform without variance through the layer. It can also be considered as the drying of one layer of sample particles or slices fully exposed to the drying air.

Thin layer drying models can be categorized into three broad groups-

1. Theoretical Equations

2. Semi-theoretical Equations

3. Empirical equations [28]

The theoretical models are derived from Fick's second law of diffusion. This model is hard to understand and difficult to use frequently. The semi-theoretical models are derived from the modification of Fick's second law and from Newton's law of cooling. Empirical models are developed from the experimental data and dimensional analysis. A brief description of these models is provided in the following sections.

2.4.2.1   Theoretical Models

Theoretical models are derived from Fick's second law of diffusion. These models are usually complex and thus not suitable for regular applications. Theoretical models involve considering too many numbers of assumptions, which makes it difficult to use but it gives a better understanding about the moisture transport processes. While empirical equation gives a better fit to the experimental data though it doesn't involve any understanding of the transport processes.

Drying processes are modeled with two main models:

(i) Distributed models

Distributed models consider both heat and mass transfer simultaneously in a drying process. It is mainly based on the interaction between time and one or more spatial variables. This physical mechanism of drying in capillary porous products is complicated, and not well understood yet. In describing the mechanism of moisture removal from

cereal grains a number of physical mechanisms have been proposed by Brooker et al. (1974) [29].

Considering these mechanism Luikov (1966, 1980) [30] developed the following equation.

$$\frac{\partial M}{\partial t} \equiv \nabla^2 k_{11} M + \nabla^2 k_{12} T + \nabla^2 k_{13} P \qquad (2.1)$$

$$\frac{\partial T}{\partial t} \equiv \nabla^2 k_{21} M + \nabla^2 k_{22} T + \nabla^2 k_{23} P \qquad (2.2)$$

$$\frac{\partial P}{\partial t} \equiv \nabla^2 k_{31} M + \nabla^2 k_{32} T + \nabla^2 k_{33} P \qquad (2.3)$$

where, M is moisture content, P is pressure and T is temperature here. k_{11}, k_{22}, k_{33} are the phenomenological coefficients, while k_{12}, k_{13}, k_{21}, k_{23}, k_{31}, k_{32} are the coupling coefficients. The pressure effect is usually far less compared with the temperature and the moisture effects, and hence can be neglected. The Luikov equations reduce to [29]:

$$\frac{\partial M}{\partial t} \equiv \nabla^2 k_{11} M + \nabla^2 k_{12} T \qquad (2.4)$$

$$\frac{\partial T}{\partial t} \equiv \nabla^2 k_{21} M + \nabla^2 k_{22} T \qquad (2.5)$$

(ii) Lumped parameter models

These models consider the effect of time alone on the dependent variables. Uniform distribution of air temperature is assumed here in the lumped element models. It does not consider the change in temperature of the product to be dried.

With this assumption, the Luikov equations become as:

$$\frac{\partial M}{\partial t} \equiv \nabla^2 k_{11} M \qquad (2.6)$$

$$\frac{\partial T}{\partial t} \equiv \nabla^2 k_{22} T \qquad (2.7)$$

Phenomenological coefficient k_{11} is known as effective moisture diffusivity (D_{eff}) and k_{22} is known as thermal diffusivity (α). For constant values of D_{eff} and α, Equations (2.6) and (2.7) can be rearranged as:

$$\frac{\partial M}{\partial t} \equiv D_{ef}\left[\frac{\partial^2 M}{\partial x^2} + \frac{a_1}{x}\frac{\partial M}{\partial x}\right] \tag{2.8}$$

and

$$\frac{\partial T}{\partial t} \equiv \alpha\left[\frac{\partial^2 T}{\partial x^2} + \frac{a_1}{x}\frac{\partial T}{\partial x}\right] \tag{2.9}$$

where, parameter $a_1 = 0$ for planar geometries, $a_1 = 1$ for cylindrical shapes and $a_1 = 2$ for spherical shapes [31].

In most of the cases, the thermal diffusivity is larger compared to moisture diffusivity. Thus, neglecting the temperature gradient, the equation leads to

$$\frac{\partial M}{\partial t} \equiv \nabla^2 k_{11} M \tag{2.10}$$

Where k_{11} is called the diffusion coefficient D_{ef}, Which can be written as,

$$\frac{\partial M}{\partial t} = \nabla(D_{ef}\nabla M) \tag{2.11}$$

The solution to this equation is based on the geometry of the material.

In literature the analytical solution to the Equation)2.11) an be found for variously shaped objects like rectangular, spherical and cylindrical bodies [32].

For infinite slab geometry, the solution is

$$MR = \frac{(M_t - M_{eq})}{(M_i - M_{eq})} = \frac{8}{\pi^2}\sum_{n=1}^{\infty}\frac{1}{(2n+1)^2}exp(-(2n+1)^2\pi^2\frac{D_{ef}\,t}{4L^2}) \tag{2.12}$$

where MR is moisture ratio, t is time, and L is the half−thickness of the slab if the evaporation takes place on both sides of the infinite slab used.

For the case of drying of a spherical body with constant radius r_o, the solution can be written as mentioned

$$MR = \frac{(M_t - M_{eq})}{(M_i - M_{eq})} = \frac{6}{\pi^2}\sum_{n=1}^{\infty}\frac{1}{n^2}\exp(-n^2\pi^2\frac{D_{ef}\,t}{r_0^2}) \tag{2.13}$$

where r_o is the radius of the sphere.

2.4.2.2 Semi-theoretical Models

Semi-theoretical models are usually the simplified general series solution of Fick's second law of diffusion. Semi-theoretical models have been developed to overcome the complexities of the theoretical models. It is easier to use and to fit the drying data of the material to be dried. It does not consider the shape of the materials. These models are generally based on Newton's Law of Cooling applied to mass transfer and need some simplifications. For example, isothermal condition is assumed and resistance to moisture transfer is considered to be confined only on the surface of the product.

These models are valid only within the temperature, relative humidity, air velocity and moisture ranges at which the models have been developed. Some commonly used and popular models are Logarithmic, the Henderson and Pabis, Lewis, Page etc. These models are simpler and easy to understand, compared to theoretical models.

Semi-theoretical models can be classified according to their derivation into following categories:

(i) Derived from Newton's law of cooling:

These models are derived by analogues with Newton's law of cooling. It can be classified in sub-groups as:

      a. Lewis model

      b. Page model & modified forms

(ii) Derived from Fick's second law of diffusion:

These Semi-theoretical models are derived from Fick's second law of diffusion. These models can be classified in sub-groups as:

      a. Single term exponential model and modified forms

      b. Two term exponential model and modified forms

      c. Three term exponential model

The Models Derived by analogy with Newton's law of cooling:

This model is analogous with Newton's law of cooling so many investigators named this model as Newton's model.

a) Newton's model

Lewis (1921) [10] first observed the similarity between the phenomena of Newton's law of cooling and the drying process of porous hygroscopic materials. He suggested that the drying rate specially during the falling rate period is proportional to the instantaneous difference in moisture content of the sample with the expected equilibrium moisture content at the end of the drying process.

Materials to be dried has been assumed to be of thin thickness. Also, drying conditions (temperature, relative humidity) have been assumed to be constant throughout the process with high air velocity.

This law can be stated as

$$\frac{dM}{dt} = -k(M - M_{eq})$$ (2.14)

where, k is the drying constant (s^{-1}).

If k is independent of M, then Equation (2.14) can be rewritten as:

$$MR = \frac{(M_t - M_{eq})}{(M_i - M_{eq})} = exp\,(-kt)$$ (2.15)

where, MR is moisture ratio, t is drying time, M_t, M_{eq}, M_i, are moisture content at any time, equilibrium and initial, respectively. k is the drying constant (s^{-1}) that can be obtained from the experimental data. This equation is known as the Lewis (Newton) model.

b. Page Model

Page (1949) [11] modified the Lewis model by adding a dimensionless empirical constant (n).

$$MR = \frac{(M_t - M_{eq})}{(M_i - M_{eq})} = exp\,(-kt^n)$$ (2.16)

where, n is a dimension and usually referred to as the model constant. This model was applied to model drying behavior of shelled corns.

c. Modified Page Model

Overhults et al. (1973) [33] modified the Page model to describe the drying of soybeans.

This modified form is generally known as the Modified Page model:

$$MR = \frac{(M_t - M_{eq})}{(M_i - M_{eq})} = exp(-kt)^n \qquad (2.17)$$

In addition, White et al. (1978) [34] used another modified form of the Page model to describe the drying of soybeans. This form is generally known as the Modified Page-I Model:

$$MR = \frac{(M_t - M_{eq})}{(M_i - M_{eq})} = exp(-(kt)^n) \qquad (2.18)$$

Diamente and Munro (1993) [35] used a different modified form of the Page model for the drying of sweet potato, which is known as the Modified Page equation-II Model:

$$MR = \frac{(M_t - M_{eq})}{(M_i - M_{eq})} = exp-k(\frac{t}{l^2})^n \qquad (2.19)$$

where, l is an empirical constant (dimensionless).

The Models Derived from Fick's Second Law of Diffusion:

a. Henderson and Pabis (Single term) Model

For infinite slab geometry, we got the modified Fick's law as:

$$MR = \frac{(M_t - M_{eq})}{(M_i - M_{eq})} = \frac{8}{\pi^2} \sum_{n=1}^{\infty} \frac{1}{(2n+1)^2} exp(-(2n+1)^2 \pi^2 \frac{D_{ef} t}{4L^2}) \qquad (2.12)$$

In semi-theoretical models, simplification of solution series to Fick's law is used to describe the thin layer drying. For slurry like algae, thin layer spread has been considered as one of the options for rapid drying and hence the solution of Fick's law for slab geometry becomes relevant. For long dehydration periods, a limiting form of above Eq. is obtained by considering only the first term in the series expansion. Then, the Eq. can be written in the following form,

$$MR = \frac{(M_t - M_{eq})}{(M_i - M_{eq})} = \frac{8}{\pi^2} exp(-\pi^2 \frac{D_{ef} t}{4L^2}) \qquad (2.20)$$

The effective diffusivity, D_{ef} is a lumped parameter resulting from the contribution of all mass transport mechanisms like gas diffusion, capillary flow, and bound water migration occurring in different phases [36].

Although transport properties like liquid diffusivity, thermal conductivity are necessary to fully describe the drying kinetics of materials, a single drying constant k, combining the effect of the various transport phenomena, is most commonly used in semi-theoretical models. Hence the first term of previous Eq. can be approximated to the form-

$$MR = \frac{(M_t - M_{eq})}{(M_i - M_{eq})} = a \, exp(-kt) \qquad (2.21)$$

where, a is defined as the indication of shape and generally named as model constant (dimensionless). These constants are obtained from experimental data. The above equation is called Henderson-Pabis model. This model has been used to predict the drying constant of corn, wheat and peanut. The slope of this model, k is related to diffusivity when drying process takes place only in the falling rate period and liquid diffusion controls the process which is typical in drying of agricultural products [37].

b. Logarithmic (Asymptotic) Model

A new model based on logarithmic form of Henderson and Pabis model after addition of an empirical term was proposed by Chandra and Singh (1995) [12].

$$MR = \frac{(M_t - M_{eq})}{(M_i - M_{eq})} = a \, exp(-kt) + c \qquad (2.22)$$

where, c is a dimensionless empirical constant

c. Midilli Model

Midilli et al. (2002) [13] proposed a modification of the Henderson and Pabis model. Their model includes an exponential term and a linear term. This model was applied to the drying of pollen, mushroom, and shelled/unshelled pistachio.

$$MR = \frac{(M_t - M_{eq})}{(M_i - M_{eq})} = a \, exp(-kt) + b * t \qquad (2.23)$$

where, b is an empirical constant (s−1)

2.4.2.3 Empirical Models

Empirical models are based on experimental data and dimensionless analysis. They are developed from the fit to different experimental data. To develop an empirical model various empirical equations are used to simulate the kinetics of mass transfer (moisture) as a function of different initial condition of the drying process [38]. The parameters used

in these models have no physical meaning, which makes it difficult to understand. They cannot give idea about the phenomena happening during the drying time. Among the models some are being used frequently than others. Thompson model, Wang and Singh model are used very commonly. The major limitation of empirical models is their dependency on experimental data only, which does not necessarily provide any information on the heat and mass transfer phenomena in the drying process.

a. Thompson Model

Thompson et al. (1968) [39] proposed a model for drying of shelled corns at the temperature range 60 -150 °C

$$t \ = \ a\,ln\,(MR) \ + \ b\,[ln\,(MR)]^2 \qquad\qquad (2.24)$$

where, a and b were dimensionless constants. This model has also been used to describe the drying characteristics of sorghum [40].

b. Wang and Singh Model

Wang and Singh (1978) [41] developed a model for intermittent drying of rough rice.

$$MR \ = \ 1 + bt + at^2 \qquad\qquad (2.25)$$

where, unit of b is in s^{-1} and a is in s^{-2}. They are constants obtained from experimental data.

c. Kaleemullah Model

Kaleemullah (2006) created an empirical model that included MR, T, and t. They applied it to the drying of red chilies[42].

$$MR \ = \ exp[-(at+b) * T^{(ct+d)}] \qquad\qquad (2.26)$$

where, a, b, c and d are model constants. Both c and d are dimensionless. A summary of the semi-theoretical and empirical models is presented in Table 2.4.

Table 2.4: Some popular isothermal drying kinetics model [28]

Serial No	Model Name	Model Equation
1	Newton/Lewis	$MR=exp(-kt)$
2	Page	$MR=exp(-kt^n)$
3	Modified Page	$MR=exp[(-kt)^n]$
4	Modified Page II	$MR=exp\left(-k\left(\frac{t}{l^2}\right)^n\right)$
5	Modified Page III	$MR=k\ exp\left(-\frac{t}{d^2}\right)^n$
6	Henderson and Pabis	$MR=a\ exp(-kt)$
7	Logarithmic	$MR=a\ exp(-kt)+c$
8	Two Term	$MR=a\ exp(-k_0t)+ b\ exp(-k_1t)$
9	Two Term Exponential	$MR=a\ exp(-kt)+ (1-a)\ exp(kat)$
10	Wang and Singh	$MR= M_o+at+bt^2$ $MR= 1+at+bt^2$
11	Midilli et al.	$MR= a\ exp(-kt^n) +bt$

2.5   Necessity of further study regarding drying

Microalgae is a promising source of raw materials for various chemicals, supplements and energy production. It can be a good alternative to conventional sources in respect of economic, environmental and sustainable point of view.

Usually, microalgae contain around 70 to 90 wt% of moisture on wet basis. As microalgae is a perishable item, it needs to be dried to preserve it. To use microalgae as a source of raw materials for chemical, nutritional or energy production, drying is a crucial step of the whole process. Drying also increase the higher calorific value and reduce transportation cots with longer storage time.

Drying steps consists of almost 75% of total cost for the production of products out of microalgae [24]. It can be noted that extensive research has been done on different options

for steps starting from algae harvest to dewatering (concentrations of 20% solids). But, drying step has not been studied thoroughly [43, 44].

From the energy balance, it can be concluded that drying of algae requires at least 60% of the energy content stored in algae. As detail study on drying step has not been done yet, there is a great chance to minimize the energy requirement. To reduce the energy requirement and to know the importance of drying step in biomass production chain, detail study of drying is essential.

To assess the energy requirement of drying process and to develop a low-cost, efficient drying system, knowledge of drying kinetics is a must. It is also an important part of developing new drying process for any material. This study involves the mechanism and the effect of different variables on moisture removal process [45].

2.6   Selection of drying models for the current study

The main mechanism of moisture transfer to the surface is believed to be diffusion process. Semi-theoretical models derived from Fick's second law are easier to solve and require much less time compared to theoretical models. They also do not need assumptions of conductivity, mass diffusivity and geometry and provide some understanding of the transfer process.

As discussed earlier, the semi-theoretical models are mainly derived from the theoretical model (Fick's second law of diffusion) or its simplified variation (Newton's law of cooling). Two models of each category have been considered here. Only the simplest forms were used to keep the work easily understandable and easier to predict the behavior.

Newton model, also known as Lewis model is the simplest model because of the model constant and the simplest form. It is derived from the Newton's law of cooling. Page model is an empirical modification of this Newton model. In Page model the errors occurred while using newton model are greatly minimized by using a new empirical dimensionless model constant (n). On the other hand, Henderson and Pabis model which is the first term of the solution of Fick's second law of diffusion. Again, a Logarithmic model is a modified form of Henderson and Pabis. These four models, namely Newton model, Page model, Logarithmic model and Henderson and Pabis model have therefore been selected for the current study.

3. MATERIALS AND METHODS

3.1 Materials

This section covers all the materials used for the research work.

3.1.1 Microorganism

Microorganism used in this study was *Chlorella vulgaris* (UTEX 2714). This strain of green algae was selected due to its relatively high lipid productivity, ability to survive shear stress, high CO2 sinking capacity, low nutrient requirement, fast growth rate and high photosynthesis efficiency [46]. The strain has been cultured at Bangladesh Council of Scientific and Industrial Research (BCSIR).

3.2 Methods

All the process that has been followed in this work have been discussed in the following sub-sections.

3.2.1 Algae production

This section discusses the procedure followed in the cultivation of *C. vulgaris*.

3.2.1.1 Preparation of growth medium

Bristol medium[1] was used for the algal growth. A stock solution of each salt was prepared by dissolving required amount of chemicals. The weight of the salt used for this purpose is shown in Table 3.1. The pH of the stock solution was set on 6.5 using 0.01N of Sodium hydroxide (NaOH) or Hydrochloric acid (HCl). Double distilled water was used for all the processes.

Table 3.1: Growth medium preparation

Salt	Stock (g/L)	Quantity from Stock (ml/L)
Sodium Nitrate ($NaNO_3$)	25	10
Calcium Chloride ($CaCl_2.2H_2O$)	2.5	10
Magnesium Sulphate ($MgSO_4.7H_2O$)	7.5	10
Dipotassium Hydrogen Phosphate (K_2HPO_4)	7.5	10

---

[1] http://web.biosci.utexas.edu/utex/Media%20PDF/bristol-medium.pdf

Potassium Dihydrogen Phosphate (KH_2PO_4)	17.5	10
Sodium Chloride (NaCl)	2.5	10
Micronutrients	-	1
Sprint 330 (Na.DTPA.Fe(III))	0.35	10

Table 3.2: Micronutrient stock solution preparation

Micronutrient Salt	Stock Solution (g/1000ml)
Zinc Sulphate ($ZnSO_4.7H_2O$)	8.82
Manganese Chloride ($MnCl_2.4H_2O$)	1.44
Molybdenum Trioxide (MoO_3)	0.71
Copper Sulphate ($CuSO_4.5H_2O$)	1.57
Cobalt Nitrite ($CoNO_2.6H_2O$)	0.49

All the stock solutions were sterilized by autoclaving 15 minutes at 121°C temperature and 1-2 bar pressure separately to avoid formation of precipitation (specially, iron and phosphate) and was added aseptically afterwards. Stock solutions were added in quantities as shown in Table 3.1 to a 1000 mL double distilled water to make 1L of Bristol medium. The concentrations of individual micronutrients are shown separately in Table 3.2.

3.2.1.2 Algae Cultivation for Biomass

The culture obtained from UTEX was in Proteose Medium. At first, the algae were transferred to Bristol media. The culture was transferred to 1L bottle containing Bristol media and after two weeks it was transferred to a 2L photo bioreactor. Bioreactor operated on a regular basis with continuous measurement of growth.

3.2.1.3 Experimental Setup

For production of *Chlorella vulgaris*, a 2L photo bioreactor (Shown in Appendix) was used. The bioreactor was obtained from the University of Texas, Austin. The photo-bioreactor contains fully adjustable red (626 nm), green (525 nm), and blue (470 nm) LED lights with total 43,200 millicandela (MCD) output. It was operating on a cycle of 12 hrs. on and 12 hrs. off. The culture was expanded in plastic bottles used in packaging of drinking water, collected from local market; glass chamber generally used for

aquarium; vertical table top photo bioreactor tube etc. Some of the pictures of the reactors have been shown in APPENDIX section.

3.2.1.4 Harvesting of Algae

After production, algae were harvested by sedimentation. The culture was kept without aeration for about six hours, then culture media was removed and the algae were collected from bottom. The algae were taken on piece of cloth and was hand-pressed to remove water from it.

3.2.2 Characterization of algal biomass

In general, algal biomass characterization involves proximate and ultimate analysis. The proximate and ultimate analysis provide detailed understanding about its characteristics. It involves the determination of moisture, volatile matter, ash fixed carbon content and also carbon, nitrogen, hydrogen, oxygen and sulfur content of the sample. In available literature, ultimate and proximate analyses have been among the most recurrently conducted tests for investigating algal biomass.

3.2.2.1 Proximate Analysis

Proximate analysis was done at Chemical Engineering Laboratory of BUET. For proximate analysis the freshly harvested algae were dried for three hours at 75 $^{\circ}$C.

3.2.2.1.1 Moisture Content/ Moisture Content

ASTM E 871 was followed to measure moisture content. Algae sample was taken in a petri dish and the weight of wet sample was calculated by subtracting the weight of empty petri dish from it. Then the petri dish with sample was kept at 105 $^{\circ}$C for 1 hour. After that, the weight of dried sample was measured like before by subtracting the weight of empty petri dish. Thus, the moisture content of Algae was measured.

$$M = \frac{w \times 100}{w_s} \qquad (3.1)$$

where M is moisture content, w is amount of water evaporated, w_s is weight of wet sample.

3.2.2.1.2 Volatile Content

For measuring volatile content ASTM E 872 was followed. At first, empty crucible was weighted and then with wet sample. The difference gave the weight of wet sample. After

that, the crucible with sample was kept in an oven at 950 ± 20 ºC for around 7 minutes. Difference with the empty crucible gives the remaining dust content. Subtracting from wet sample weight, total volatile content was calculated.

$$V = \frac{v \times 100}{w}$$)3.2(

Where V=Volatile content, v= amount of volatile; w= weight of wet sample

3.2.2.1.3 Ash Content

Standard procedure for Ash content measurement described under ASTM D 1102 was followed. In the beginning, empty crucible was weighted and then again with wet sample. The difference gave the weight of wet sample. After that, the crucible with sample was kept in an oven at 600 ºC for 20 minutes. Difference with the empty crucible gives the amount of ash. Using this data total ash content was calculated.

$$A = \frac{a \times 100}{w}$$ (3.3)

Where A=Ash content; a= amount of ash; w= weight of wet sample

3.2.2.1.4 Fixed Carbon

Instructions followed for measuring amount of fixed carbon was taken from ASTM E 870. In this method, the sum of moisture content, volatile and ash content was subtracted from 100 to get the amount of total fixed carbon.

$$Fixed\ carbon = 100 - (Moisture\ Content + Volatile + Ash\ Content)\ (3.4)$$

3.2.2.2 Ultimate Analysis

Ultimate analysis helps to understand the effectivity of microalgae as a bio-fuel producer [80]. The prospective value of any biomass as a bio-fuel feedstock is largely governed by physicochemical properties of the molecules from which it is constituted. Various properties such as calorific value, elemental composition, bulk density, ash content, moisture content, volatile matter content etc. affect the performance of a biomass fuel and as such proper determination of these properties is a must for choice of conversion technologies.

3.2.3 Calorific Value

ASTM E 711 was followed for the measurement of calorific value of the sample. A bomb

calorimeter was used for this purpose. The bomb calorimeter was charged with oxygen of around 25 bar pressure. Sample was taken in the empty crucible after taking its weight. A copper wire was set inside the crucible to make fire when the electric supply is on. Initial temperature was recorded and the electric circuit was turned on making the fire inside the calorimeter. The temperature started to rise and final temperature was recorded. With these data calorific value of the sample was calculated by using Equation (3.5)

$$CV = [(mCp)_b + (mCp)_w]\Delta T - (mu)_c)/m \tag{3.5}$$

Where, CV= Calorific value;

Energy equivalent factor of the calorimeter = $(mCp)_b$ + $(mCp)_w$; Correction for fused copper wire and others = $(mu)_c$

3.2.4   Thermal Analysis

For the thermal analysis DSC, TGA were performed. The details method of those experiments along with some other assumptions have been discussed under section 3.2.4.1 to 3.2.4.3.

3.2.4.1   Differential scanning calorimetry

DSC-60 (Shimadzu, Japan) at the Centre for Advanced Research in Sciences (CARS) of the University of Dhaka was used for the differential scanning calorimetry between room temperature and 600° C. In a typical DSC experiment, the temperature of the sample unit, formed by the sample and reference material, is varied by 10 K/min, and the temperature difference between the sample and the reference

Figure 3-1: Differential scanning calorimetry (DSC-60, Shimadzu, Japan)

material was measured as a function of temperature. DSC measures the ability of the sample to release or absorb energy. The technique characterizes the endothermic and exothermic behavior of the sample material during the drying process.

3.2.4.2 Thermogravimetric Analysis

The thermogravimetric experiments were carried out in a thermogravimetric analyzer (TGA; TGA-50; Shimadzu, Japan) at CARS, University of Dhaka. In a typical run, approximately 5 mg algae sample was loaded in an aluminum cell. The sample was then heated in a 10 mL/min nitrogen flow to 600 °C at two different heating rates: 5 K/min and 20 K/min. The weight loss of the sample during the heating period was recorded. These data were used to calculate the derivate curve of weight loss, which is known as the differential thermogravimetry (DTG) curve.

3.2.4.3 Non-isothermal Drying Kinetics

In literature, drying kinetics of various biomass especially various agricultural products were usually studied under isothermal condition and many isothermal drying models have been proposed.

Figure 3-2: TGA (TGA-50, Shimadzu, Japan)

There are a lot of semi-theoretical models available in literature as mentioned in literature review section. Semi-theoretical models are generally derived by simplifying general series solution of Fick's second law and Newton's law of cooling as discussed earlier. Four models were chosen for analysis the data to compare the drying kinetics of *Chlorella vulgaris*. These models (Shown in Table 3.3) are mainly derived from the Newtons law of cooling and Fick's second law. Others are mainly the modification of these models and some are comparatively complex, were not considered for this study.

Table 3.3: Four most popular isothermal drying kinetics model

Serial No	Model Name	Model Equation	
1	Newton/Lewis	$MR=\exp(-kt)$	(2.15)
2	Page	$MR=\exp(-kt^{n})$	(2.17)
3	Henderson and Pabis	$MR=a*\exp(-kt)$	)2.21(
4	Logarithmic	$MR=a*\exp(-kt)+c$	)2.22(

The equations shown in Table 3.3, show the isothermal forms of the models. These equations were modified for the study of non-isothermal kinetics, by the introduction of a temperature dependent term. The procedure is described below.

The parameter k is the drying rate constant, which is dependent upon temperature. The temperature dependency can be expressed by Arrhenius-like relationship as shown in Equation)3.6),

$$k = k_0 exp\left(-\frac{E}{RT}\right)$$

)3.6(

where, k_0 is the preexponential factor, E is the activation energy, R is universal gas constant, and T is the absolute temperature.

As we have used non-isothermal heating, the temperature will increase with time. The time-temperature relationship for constant heating rate is shown in Equation)3.7).

$$T = T_0 + \beta t$$

)3.7(

where, T is the temperature at time t, T_0 is the initial temperature and β is the heating rate.

After substituting these two relations in the isothermal drying kinetics model, non-isothermal drying kinetics models can be obtained. The non-isothermal expressions are shown in Equation. 3.8 to 3.11 and listed in Table 3.4. These derived non-isothermal drying kinetics models were used to determine the best suited drying kinetics model for *Chlorella vulgaris*.

Table 3.4: Derived non-isothermal model along with original form

Model Name	Isothermal expression	Non-isothermal expression	
Newton/Lewis	MR=exp(-kt)	$MR = exp\left[-k_0\, exp\left(-\frac{E}{RT}\right)\frac{T-T_0}{\beta}\right]$	(3.8)
Page	MR=exp(-kt^n)	$MR = exp\left[-k_0\, exp\left(-\frac{E}{RT}\right)\left(\frac{T-T_0}{\beta}\right)^n\right]$	(3.9)
Henderson and Pabis	MR=a exp(-kt)	$MR = a\, exp\left[-k_0\, exp\left(-\frac{E}{RT}\right)\frac{T-T_0}{\beta}\right]$	(3.10)
Logarithmic	MR=a exp(-kt)+c	$MR = a\, exp\left[-k_0\, exp\left(-\frac{E}{RT}\right)\frac{T-T_0}{\beta}\right] + c$	(3.11)

3.2.5 Model Fitting

Based on the data obtained from TGA for drying, the moisture ratio was calculated using Equation)3.12)

$$MR = \frac{m_T - m_e}{m_i - m_e} \qquad (3.12)$$

Where, MR is the moisture ratio, m_T is the mass at temperature T, m_i is the initial temperature and m_e is the mass at the end of the drying process. The parameters of the non-isothermal kinetic models were obtained through non-linear regression of the experimental data . The quality of the fitted models can be evaluated with the following statistical measures: Correlation coefficient (R), coefficient of determination (R^2), Reduced chi square (χ^2), mean bias error (MBE), root mean square error (RMSE), Sum square error (SSE), modelling efficiency (EF), mean percent error (MPE), Mean square error (MSE).

The goodness of fitting was evaluated based on the value of R^2 and other criteria such as χ^2, RMSE, MBE, MPE, SSE, EF, MSE. The values of coefficient of determination R^2 can be used to test the linear relationship between experimental and model calculated values and is one of the primary criteria for the selection of best model.

In this study, the parameters used to evaluate the fitness of the non-isothermal drying behavior have been shown in Equation (3.13) and (3.14)

$$\chi 2 = \frac{\sum_{i=1}^{N}\left(MR_{exp,i} - MR_{pre,i}\right)^2}{N - z} \qquad (3.13)$$

and

$$RMSE = \sqrt{\frac{1}{N}\left(MR_{exp,i} - MR_{pre,i}\right)^2} \qquad (3.14)$$

where, $MR_{exp,i}$ is the experimental moisture ratio, N is the number of experimental data points and z is the number of parameters in the model.

4. RESULTS AND DISCUSSION

4.1 Introduction

This chapter includes a compilation of experimental findings and their analysis: proximate and ultimate compositions of *Chlorella vulgaris*; TGA, DTG and DSC curves derived from the drying behavior of *Chlorella vulgaris*; models developed from drying data and their goodness of fit. Detailed data and images have been included in the Appendix section.

All the experiments were done in triplicates and average values were used for calculation.

4.2 Proximate Analysis

Table 4.1 represents the proximate analysis of *Chlorella vulgaris*, in both wet and dry basis, obtained after 3 hours of heating at 75 ^{0} C. It shows a significant amount of volatile content present in the sample. These volatile components include different types of hydrocarbons, acids, alcohols, esters, aldehydes and ketones as well as aromatics, and nitrogen compounds (pyrroles and amides), originating from the lipid, protein, and carbohydrate fractions of the microalgae. Another significant parameter is ash content which includes total amount of iron, calcium, potassium, magnesium, sodium, phosphorus present in chlorella.

Table 4.1: Proximate analysis of *Chlorella vulgaris*

Parameter	Wet basis	Dry basis
Moisture Content	6.67 %	-
Volatile	70.51 %	75.55 %
Ash Content	15.46 %	16.56 %
Fixed Carbon	7.36 %	7.89 %

4.3 Ultimate Analysis

Results presented in Table 4.2 signifies the value of higher heating value of *Chlorella vulgaris* along with the elemental analysis showing the composition in C, H, N, S percentage.

Table 4.2: Ultimate analysis and heating value of *Chlorella vulgaris*

Element	Mass percentage
C	43.02
H	8.53
N	14.40
S	3.5
O	30.55
Higher Heating Value (Dry Basis)	*12.63 MJ/Kg*

4.4 Thermogravimetric Data Analysis

The results of the Thermogravimetric experiments have been presented in Figure 4 1, which shows the relation between the temperature and the weight loss. This weight loss is mainly due to moisture loss, volatile compounds loss and decomposition of the sample.
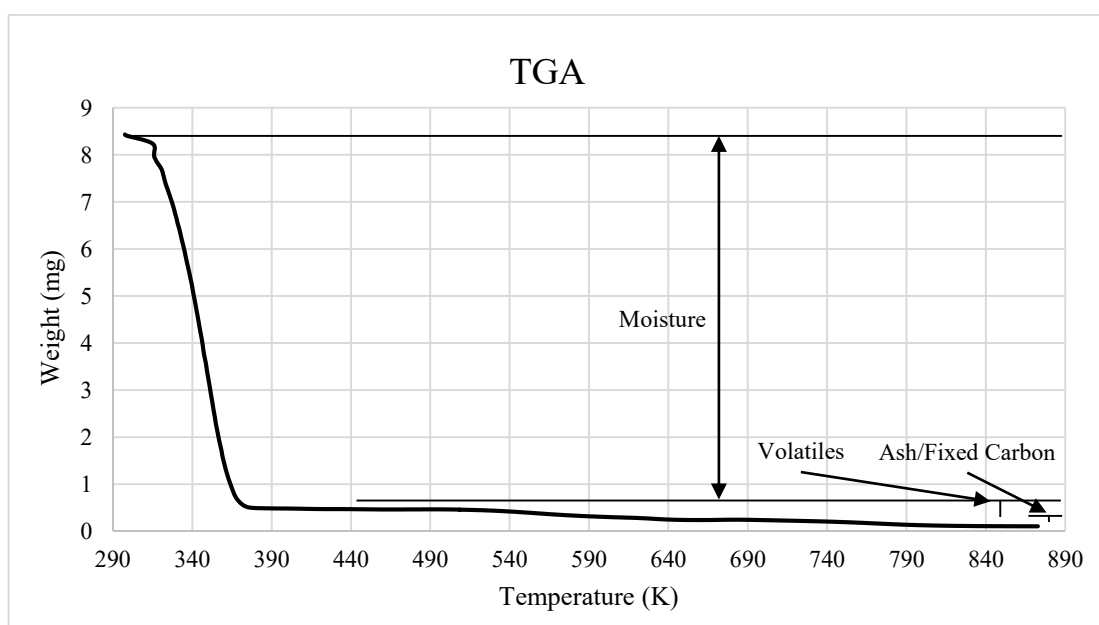
Figure 4-1: Thermogravimetric curve from temperature range of RT to 600^{0}C for

5 K/min drying rate

At the beginning the weight of the wet sample was 8.435 mg. With the increase in temperature at a linear rate of 5 K/min, a decrease of weight was observed. In the first step of mass loss (Stage I in Figure 4-2), the moisture content dropped rapidly as the temperature increased. An apparent mass loss peak was observed in the temperature range of 75°C-80°C, which due to considerable moisture evaporation.

When the temperature exceeded 150°C, the sample went through a complex thermal chemical reaction. Different volatile matter is released resulting a significant loss of mass. These components consisted of hydrocarbons, acids, alcohols, esters, aldehydes and ketones [28].
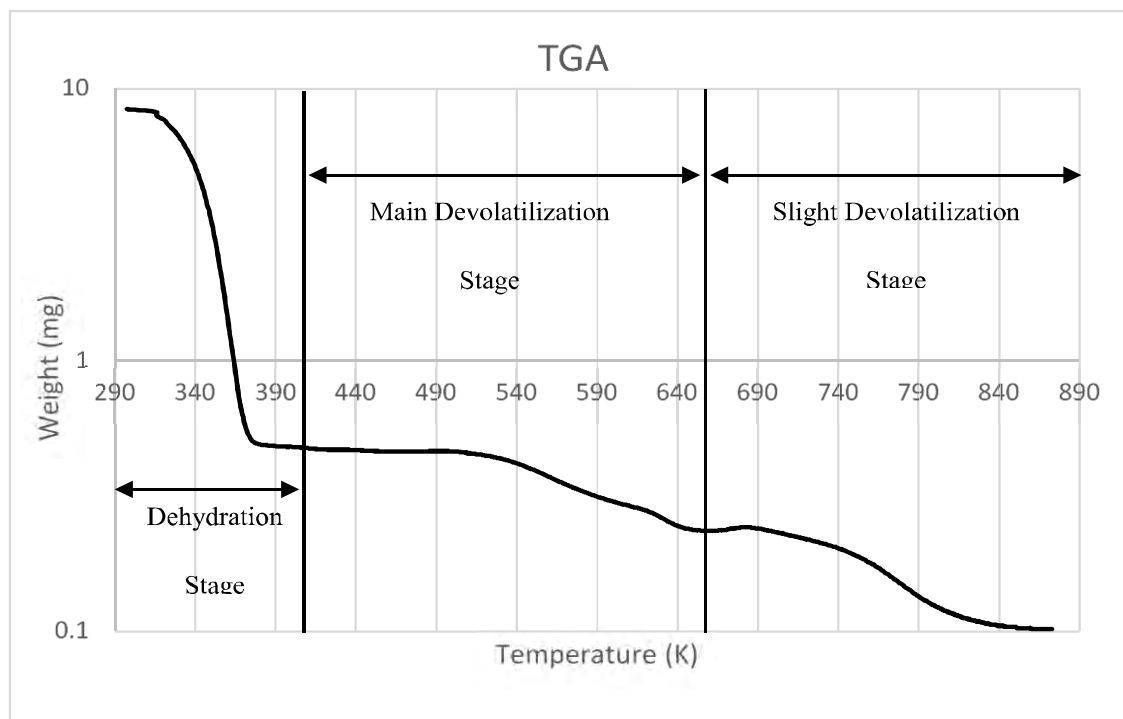
Figure 4-2: Different region of drying in log-log plot

A log-log plot in Figure 4-2 shows the regions of weight loss more clearly with further heating. From this figure, different stages of drying *Chlorella vulgaris* can be easily identified. It was observed that, biomass pyrolysis process consisted of three stages: moisture evaporation (Stage I) from room temperature to 150°C, main devolatilization (Stage II) between 150°C to 390°C, and continuous slight devolatilization (Stage III) above 390°C. This experiment was done up to 600°C.

The difference between the weight at the start and the weight after the end of stage I, that means up to 150^0 C is considered as the moisture content of the wet sample. During the devolatilization stages the weight loss signifies the amount of total volatile component and at the end of the run the remaining weight represents fixed carbon/ Ash content. Figure 4-1 shows these parameters from different region of TGA curve. The data plotted in Figure 4-1 indicated that the sample contained around 94% moisture. The stage where the moisture is lost, i.e., stage I, is the main concern of this current study.
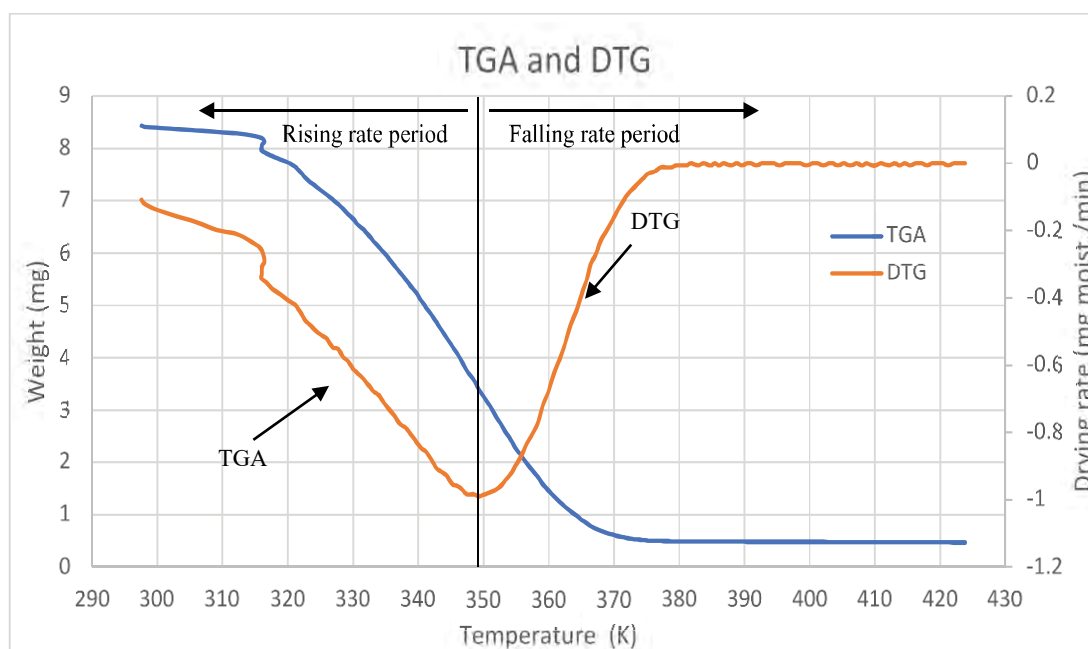
Figure 4-3: TGA and DTG showing peak point

Both TGA and DTG data were plotted in Figure 4-3. DTG curve justifies the point of highest moisture removal rate. The peak was observed at 75°C. After that, the rate falls and comes to near zero at around 423K or 150^0 C. The region up to 150^0 C involves mainly water/moisture loss from the sample. When the temperature approaches 150°C, the TGA/DTG curves became flat and the thermal decomposition of organic ingredients of biomass started. Therefore, 150 °C is generally regarded as the temperature at which dehydration ends.

It is obvious from Figure 4-1, Figure 4-2 and Figure 4-3 that the constant rate period was absent and apparent water loss peaks take place at around 75°C. Therefore, taking the water loss peak as the demarcation point, the moisture evaporation stage can be divided into rising rate period and falling rate period as shown in Figure 4-3.

The change in water loss rate is closely related to the bonding force between water and biomass. There are several types of moisture present in any moist sample. They are free water (mainly adhering to the surface of the) and bound water (present in the adsorbed condition into the pores of the sample). Free water has a weak bonding force with the materials and evaporates before the temperature reaching 90 °C.

However, bound water is distributed inside the materials, with strong bonding force, and would be completely separated only at the temperature above 120 °C. During the rising

rate period, free water rapidly diffuses outward under the temperature and steam pressure gradient to satisfy the need of surface water for gasification. A substantial amount of water escapes as steam and the drying rate increases rapidly. Therefore, before the appearance of the water loss peak, this drying process can be regarded as the evaporation of free water in algae.

As the drying process continues, less free water on the biomass surface is available and the bound water participates in the diffusion process. The falling rate period begins as the rate starts to decrease.. During this period, the drying rate is dominated by the moisture diffusion of the biomass. Because of the more resistance, bound water needs more time and energy to escape. When the evaporation of bound water is complete, the drying rate approaches zero.

4.4.1 Effects of heating rate on drying curves

In this study two heating rates (20 K/min, 5 K/min) were used. Increasing the heating rate shifted the mass loss curve to the left, which signifies accelerated decrease in moisture ratio.
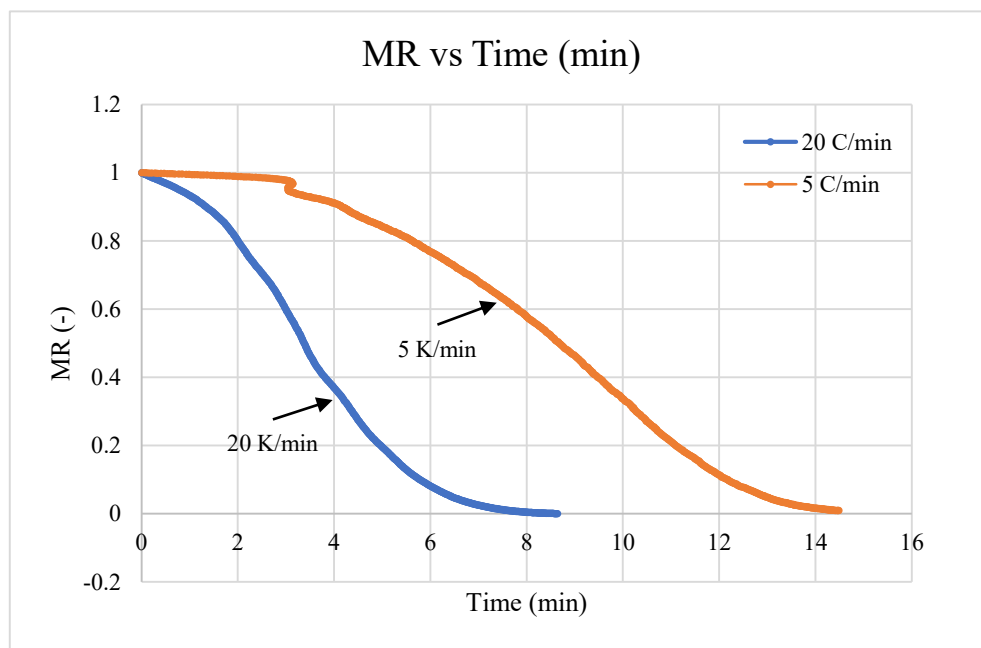
Figure 4-4: Effects of heating rate on moisture removal

Here the lowest time to reach the final moisture was observed at the heating rate of 20 K/min. Each moisture ratio loss curve showed mainly two regions. The initial region is almost close to the horizontal line (highly noticeable in 5 K/min rate curve) is the heating stage. This stage lasted for approximately 3 minutes. This was followed by a sharp fall in

moisture ratio loss. It was the main drying region. It took 8.5 to 14.5 min to end the drying process. The time required in drying at rate 5 K/min is much higher than 20 K/min. As the drying rate is slower the time would be higher, this is obvious. But, at 5 K/min drying rate the moisture removal stopped at around 100 ^{0} C, whereas it rose up to 200 ^{0} C for 20 K/min drying rate. At higher heating rates, there is not enough time for the moisture to migrate from the sample. However, at lower heating rates, there is more time for the moisture to migrate from the sample.

4.5 Model fitting

Four models were used to fit the data obtained from TGA. Three parameters were considered as the criteria to determine the best fit as mentioned earlier. These are R^2, χ2 and RMSE. R^2 value closed to 1 means better fitting. The closer to 1 the better the fit. On the other hand, for χ2 and, the less the value the better the fit.

4.5.1 Fitting of 5 K/min drying rate data:

The data fitted to the Newton model has been plotted and showed in Figure 4-5. It shows two graphs, the top one reflects the relation between the MR (Moisture Ratio) and T (Temperature). Both experimental data and data obtained from Newton model have been shown here. While the bottom graph shows the residual errors of moisture ratio predicted by the non-isothermal drying models deviating from the experimental moisture ratios. Fitting for other models are as shown in Figure 4-5 to Figure 4-8.
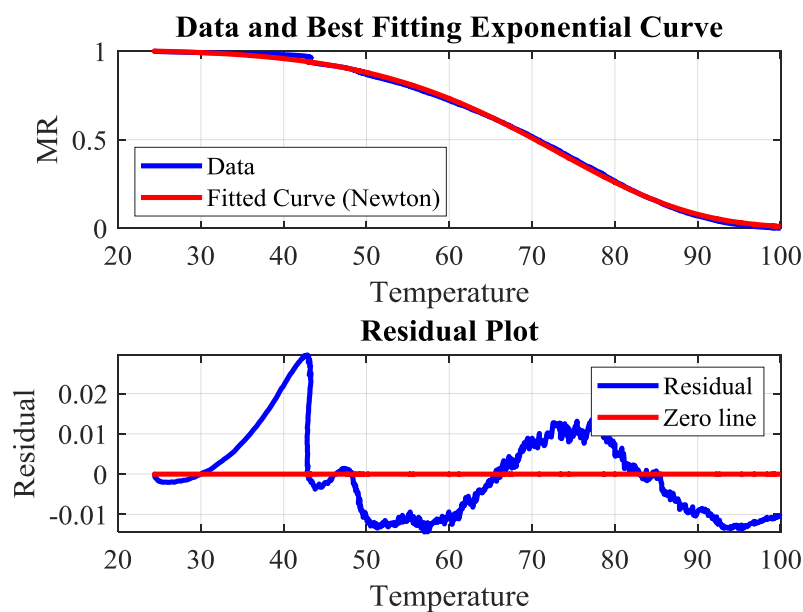
Figure 4-5: Model fit for Newton model

Data and Best Fitting Exponential Curve

Residual Plot
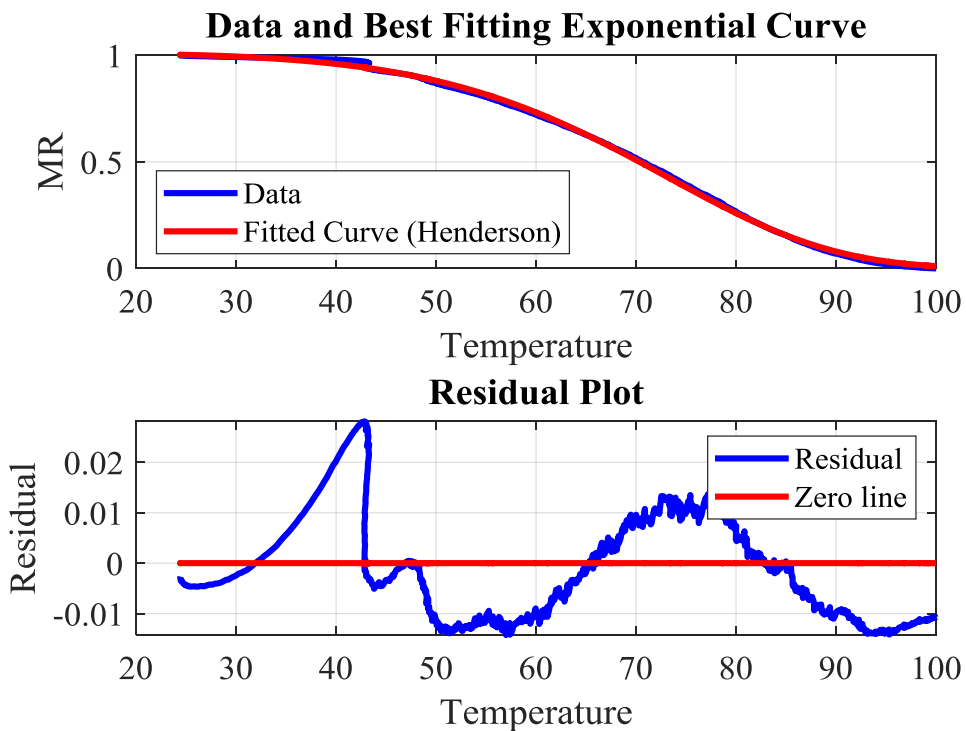
Figure 4-7: Model fit for Henderson model

Data and Best Fitting Exponential Curve

Residual Plot
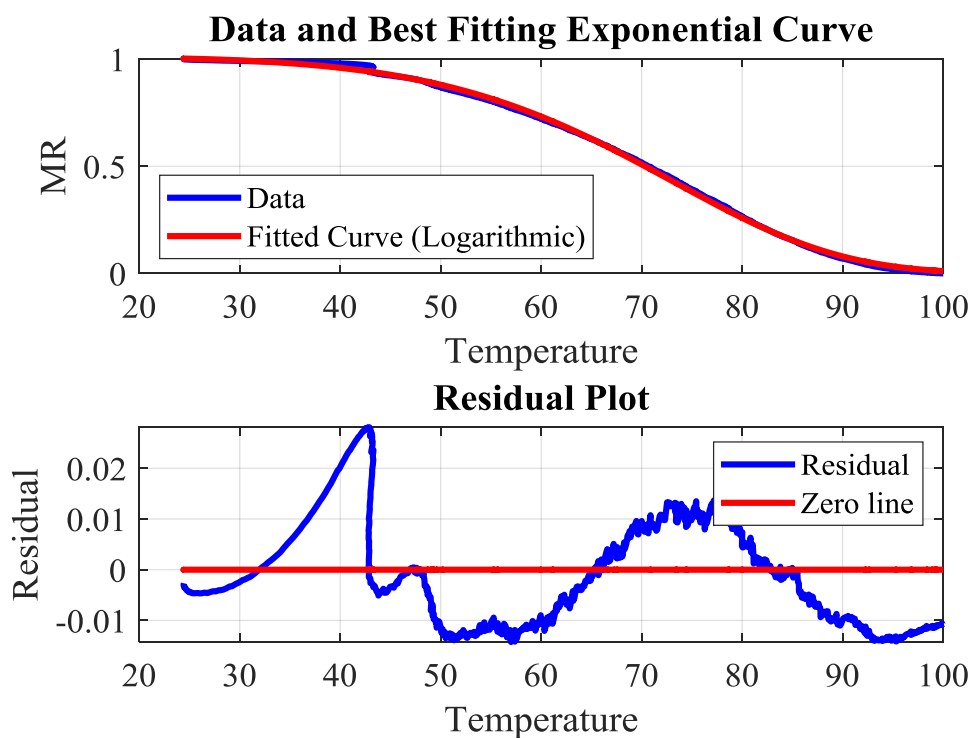
Figure 4-6: Model fit for Logarithmic model
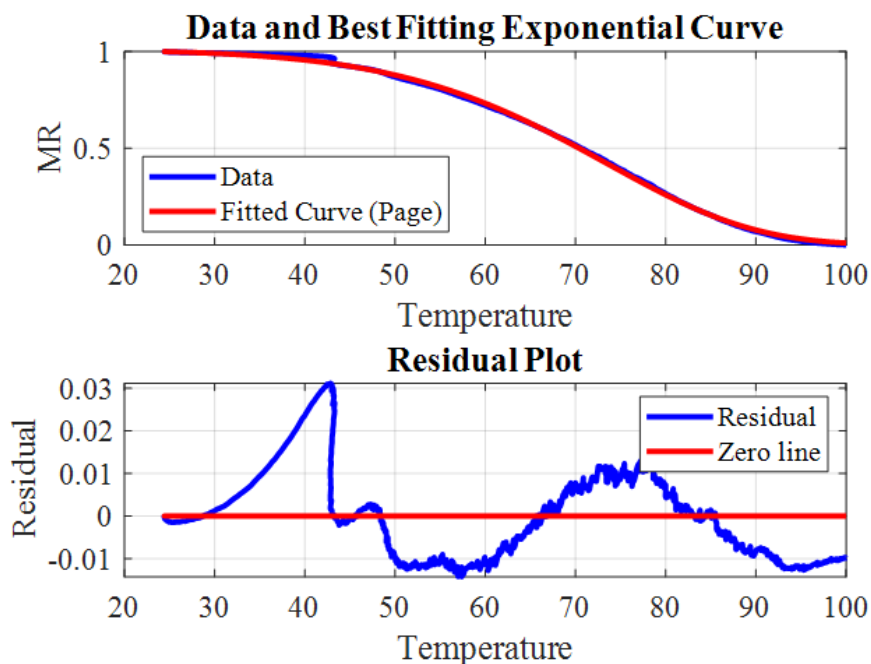
Figure 4-8 :Model fit for Page model

The list of model parameters along with the goodness of fitting values obtained from all four drying kinetics models have been shown in Table 4.3.

Table 4.3: Data showing the quality of fit using all four models

Models	R^2	χ^2	RMSE	a	c	E	k	n
				(-)	(-)	(kJ.mol^{-1})	(min^{-1})	(-)
Newton	0.999	1.117E-04	0.0106	-	-	49.87	2.89E6	-
Henderson and Pabis	0.999	1.110E-04	0.0152	1.002	-	49.46	2.52E5	-
Logarithmic	0.999	1.111E-04	0. 0105	1.003	2.33E-6	49.46	2.52E6	-
Page	0.999	1.107E-04	0.0105	-	-	52.71	1.03E7	0.873

From the data shown in Table 4.3, it can be seen that all four models show good fitting. The same thing happens for different kinds of agricultural products [26, 29, 37, 38]. Among the four, Page model shows the best fitting. **R^2** value was more closed to 1 than other three models, while having lowest value of **χ2** and **RMSE** value. Among the four models, both Page and Newton model shows the better match while Page is the most perfect one. However, the differences between the R^2 values are extremely small and hence it can be concluded that all models can fit the drying data of *C. vulgaris* well.

4.5.2 Fitting of 20 K/min drying rate data:

The fit data for Newton model has been plotted and showed in Figure 4-9.
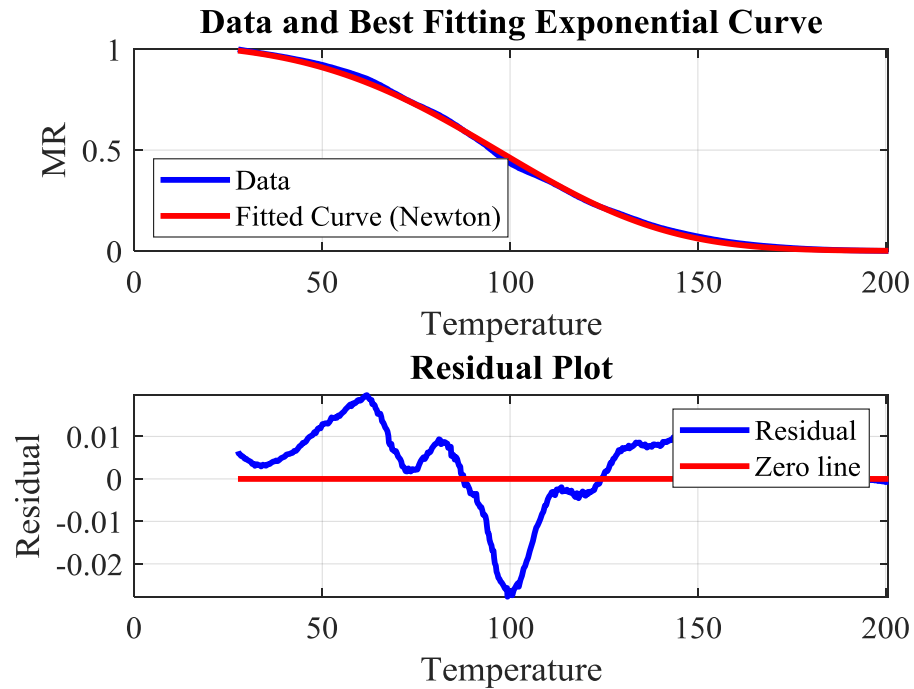
Figure 4-9: Model fit for Newton model

It shows two graphs, the top one reflects the relation between the MR (Moisture Ratio) and T (Temperature). Both experimental data and data obtained from Newton model are shown here. While the bottom graph shows the residual errors of moisture ratio predicted by the non-isothermal drying models deviating from the experimental moisture ratios. Fitting for other models are as shown in Figure 4-10 to Figure 4-12.
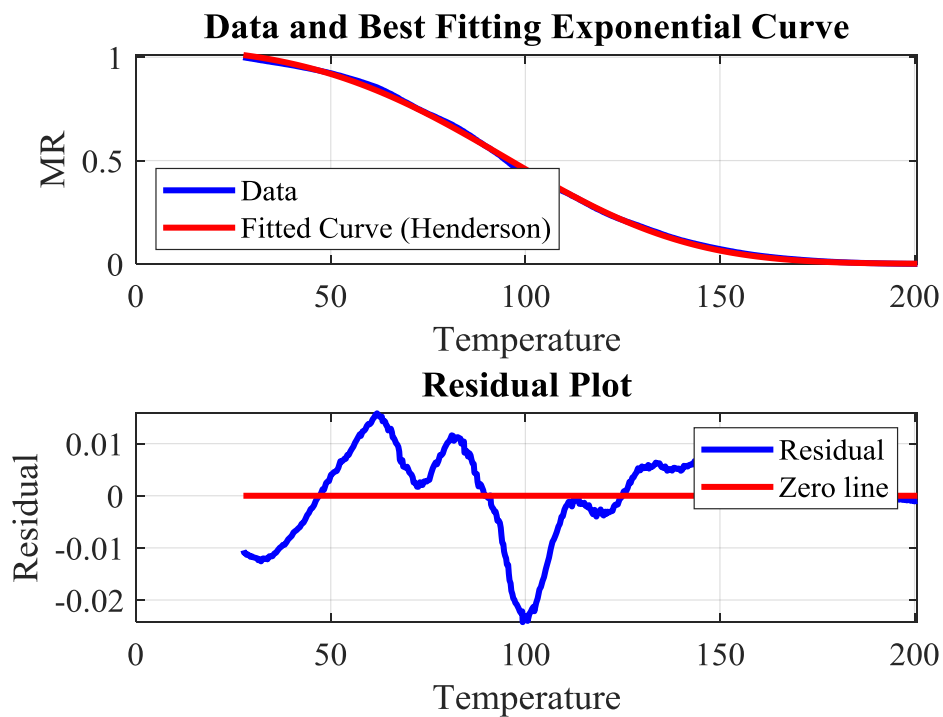
Figure 4-10: Model fit for Henderson and Pabis model
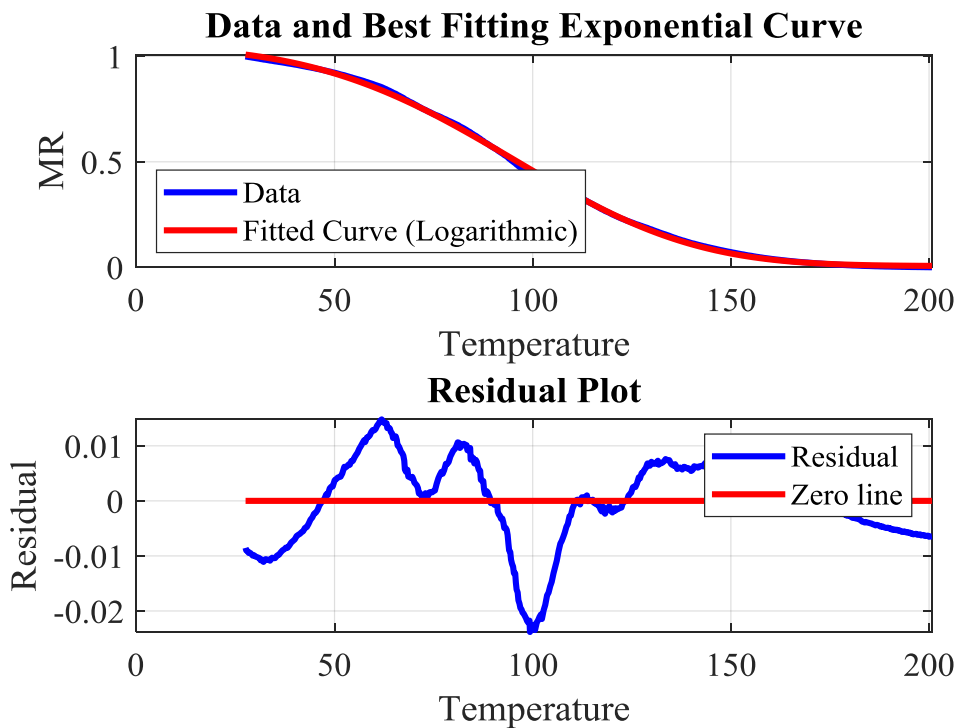
Figure 4-11: Model fit for Logarithmic model
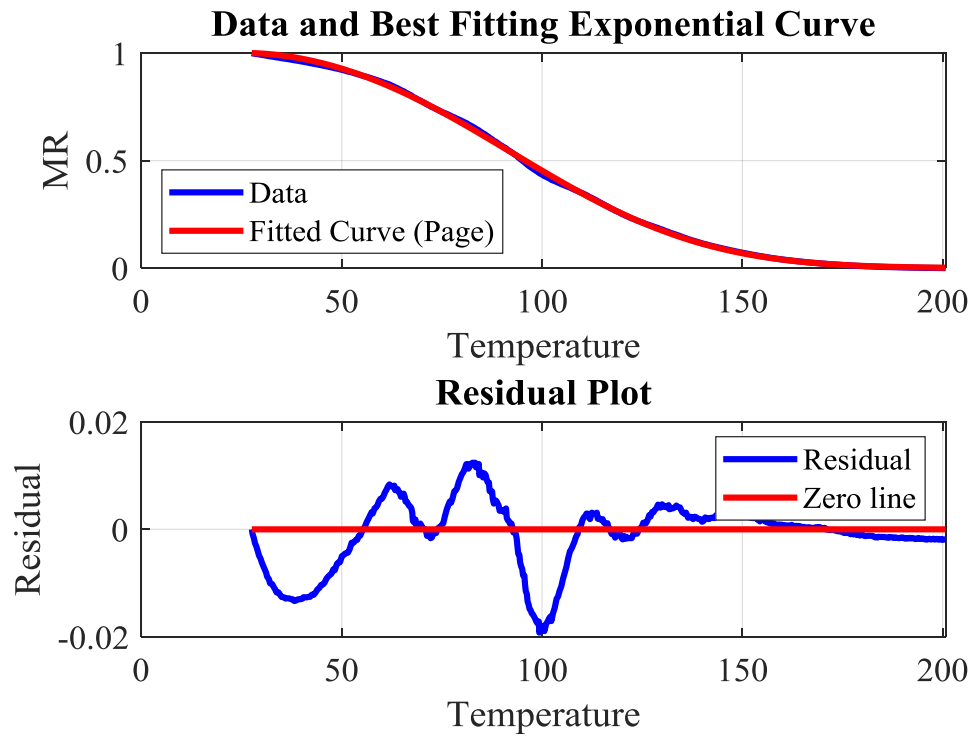
Figure 4-12: Model fit for Page model

The list of model parameters along with the goodness of fitting values obtained from all four drying kinetics models are shown in Table 4.4.

Table 4.4: Data showing the quality of fit using all four models along with calculated parameters

Models	R^2	χ^2	RMSE	a	c	E (kJ.mol^{-1})	k (min^{-1})	n
Newton	0.99939	7.588E-05	0.00869	-	-	19.62	119.58	-
Henderson and Pabis	0.99947	6.6157E-05	0.00811	1.01	-	18.98	99.02	-
Logarithmic	0.99951	6.097E-05	0.00778	1.003	5.72E-3	19.48	117.1	-
Page	0.99969	3.842E-05	0.00618	-	-	10.24	2.83	1.58

From the Table 4.4 it can be seen that all four models show good fitting. The same thing happens for different kinds of agricultural products [26, 29, 37, 38]. Among the four, Page model shows the best fitting. R^2 value was more closed to 1 than other three models, while having lowest value of $\chi 2$ and **RMSE** value. Among the four models, both Page and Newton model shows the better match while Page is the best one. However, the differences between the R^2 values are extremely small and hence it can be concluded that all models can fit the drying data of *C. vulgaris* well.

It can be concluded that in both cases, Page model fits the drying behavior very well. Data obtained from both drying rate (5 K/min and 20 K/min) can easily be predicted by this model.

4.6   Fitting of drying curve for the parameters derived from another drying rate

Two different drying rates have been used in this study. Under this section, Page equation with parameters obtained from one heating rate has been compared with the experimental value obtained at other heating rate. At first, drying curve obtained at a heating rate of 5 K/min from the experiment has been compared with values obtained from using parameters value obtained from drying curve of heating rate 20 K/min using the Page model. The comparison has been shown in Figure 4-13.
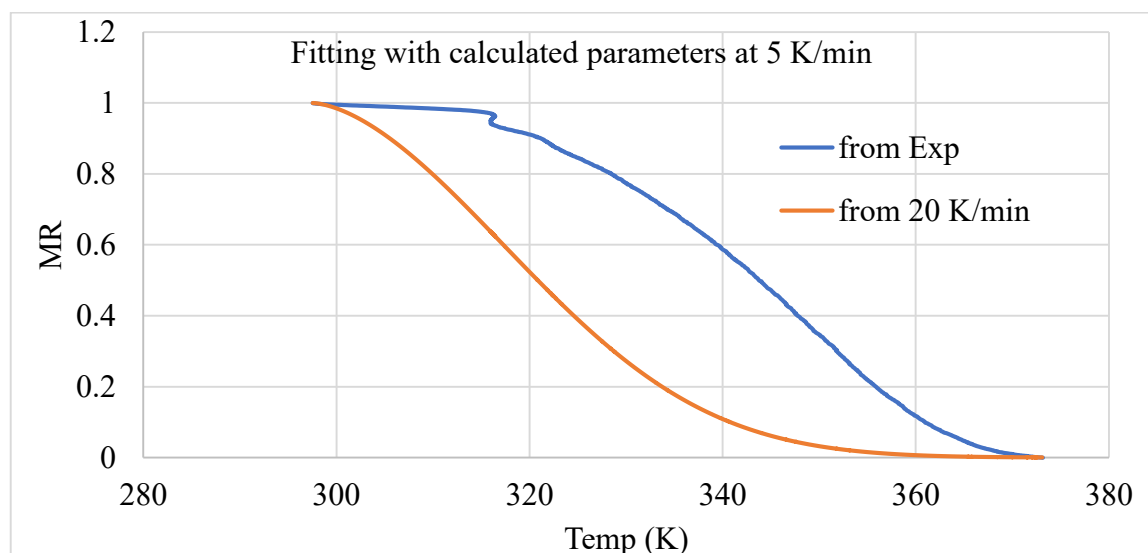
Figure 4-13: Drying curve of heating rate 5 K/min with parameters obtained from heating rate 20 K/min

It can be seen that the fittings are not good at all. So, the parameters obtained from 20 K/min heating rate has not succeed to predict the drying behavior at another heating rate.

The next plot as shown in Figure 4-14, shows the opposite combination. Drying curve of heating rate 20 K/min fitted with parameters value obtained from drying curve of heating rate of 5 K/min using the Page model.
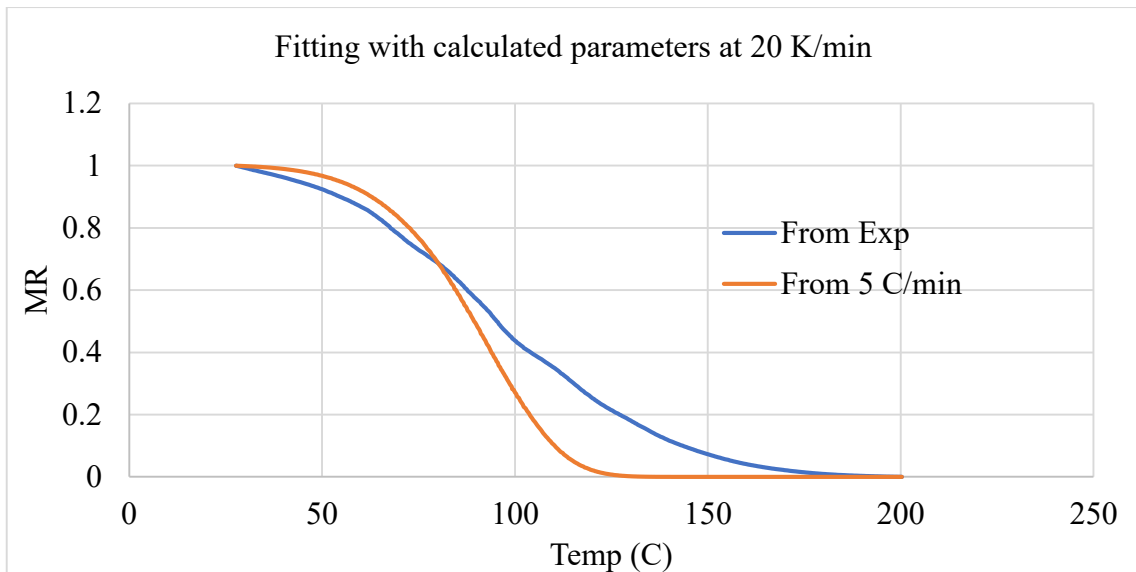
Figure 4-14: Drying curve of heating rate 20 K/min with parameters obtained from heating rate 5 K/min

From the Figure 4-13 and Figure 4-14, it can be seen that the parameters derived from one drying curve with a drying rate fails to fit the other one .This happens because drying rate has effect on drying kinetics .
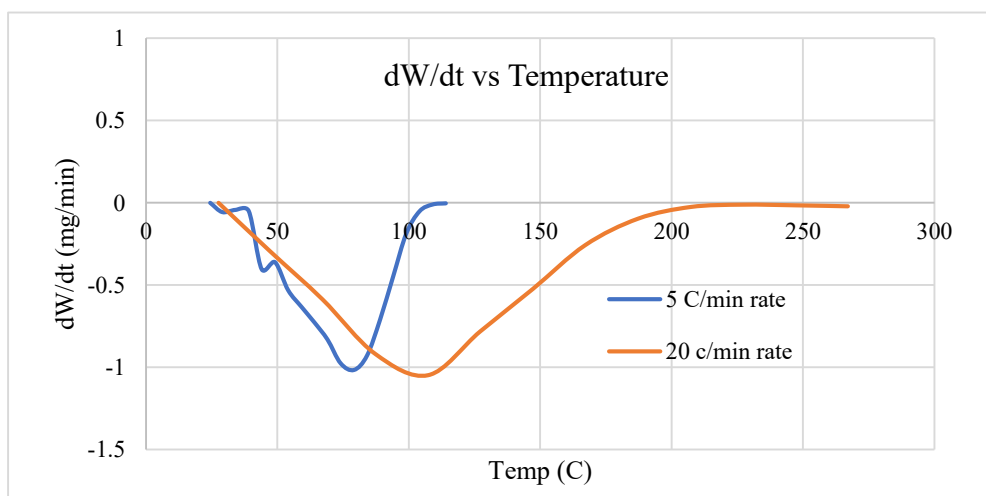
Figure 4-15: Effects of heating rate on weight loss derivative

The activation energies have been decreased with increasing heating rate. Because with rising of the heating rate, the drying period occurred toward high temperature range, which could lead to increasing the temperature inside the biomass. The weight loss derivative reached its highest value of 1.047 mg/min at the heating rate of 20 K/min at about 107 °C as seen on Figure 4-15. Because of these reason parameters derived from a drying rate does not fit the drying curve for another drying rate. Among the two graph the prediction of drying behavior for another heating rate is closer in case of low heating rate which is in this case 5 °K/min.

4.7 DSC analysis for drying

The Figure 4-16 shows the heat requirement during the drying process. The DSC curve shows two distinct peaks. The first peak is at around 42^0 C and the second one is at around 64^0 C. The first peak is mainly due to free water present in the sample.
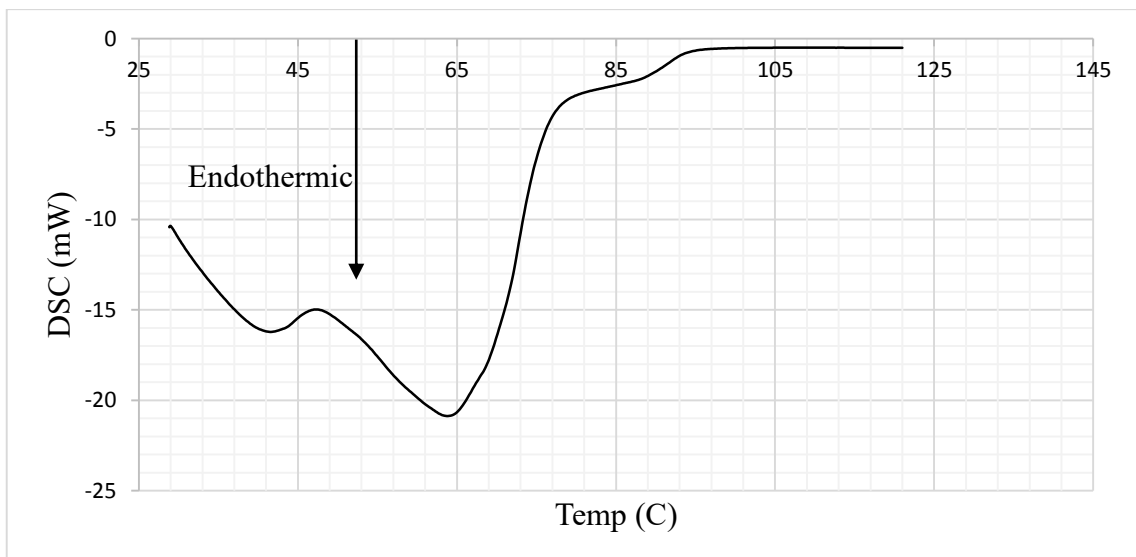
Figure 4-16: DSC curve

While after 42^0 C, not only free water but also bound water contribute to the heat requirement. Apart from these there is a shoulder at around 89^0 C.

Each peak in the DSC curve indicates a phase, in this case different phases of water. Therefore, the DSC curve indicated the presence of two or three types of moisture being present in the sample. The DSC curve is therefore fitted with three separate gaussian curves as shown on Figure 4-17.
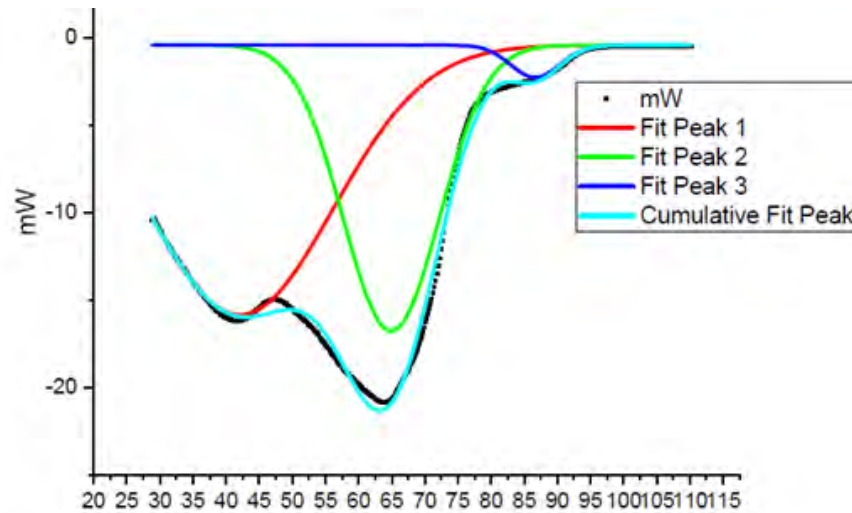
Figure 4-17: DSC curve presented by three gaussian curve

It can be seen that three curves have successfully replicated the DSC curve from the experiment. So, The presence of three types of moisture present can be assumed. Types of moisture can further be investigated by TGA data analysis. Three gaussian curves were selected to represent three types of moisture. Newtons model was considered for the purpose. The fittings of calculated data with experimental data have been shown in Figure 4-18.
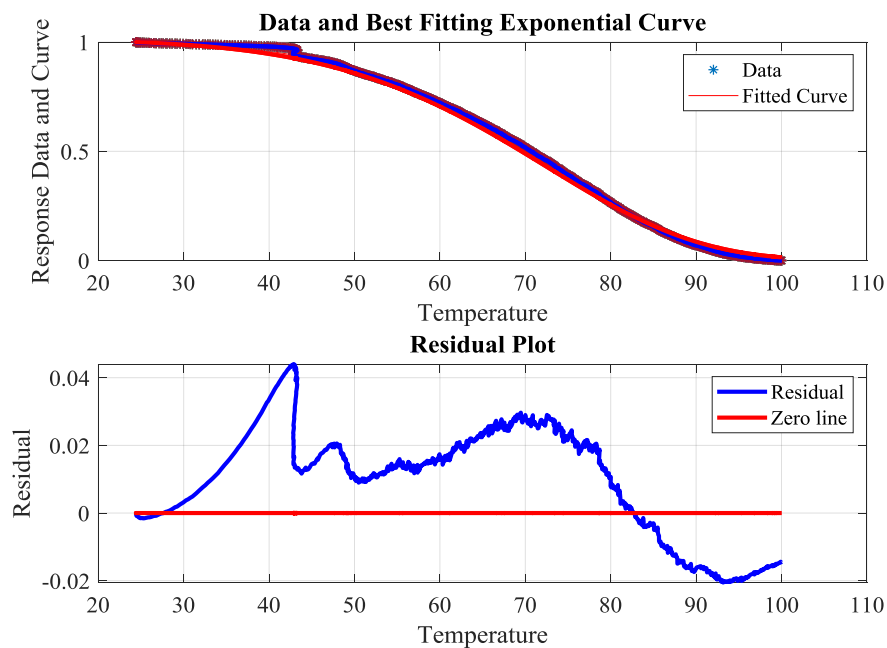
From the Figure 4-18 it can be seen that the matching is quite good. The results of the parameters along with their contribution has been shown on Table 4.5.

Table 4.5: Data for three curve fit.

Moisture Type/Region	E	K	%	R² value
Curve 1	45.54	6.628429 E05	0.9892	
Curve 2	13.79	1.475588e E06	0.0001	0.9971
Curve 3	25.09	1.964289 E03	0.0107	

The R square value of the fit is 0.9971. From the Table 4.5, it is apparent that the contribution of all three curves is not the same. The results show the maximum contribution is coming from curve 1. Another fit was plotted considering only two regions. The result has been shown as follows in Figure 4-19.
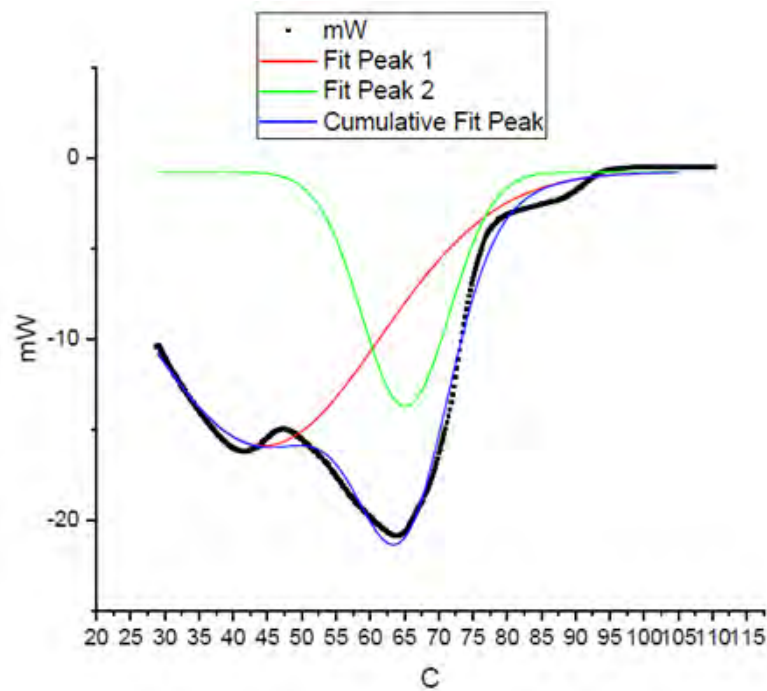
Figure 4-19: DSC curve presented by two gaussian curve.

Similarly, it can be seen that two curves have successfully replicated the DSC curve from the experiment here too. So, it can be assumed the presence of two types of moisture present. Types of moisture can further be investigated by TGA data analysis. Two equations were selected to represent two types of moisture. Newtons model was considered for the purpose too. The fittings of calculated data with experimental data are

as follows. Also, the fact was verified with two equation fit and the plot data is presented in Table 4.6.

Table 4.6: Data for two curve fit.

Moisture Type/Region	E	k	%	R²
Curve 1	49.87	2.8929E05	0.999	0.9939
Curve 2	3.56E3	3.6106E06	0.001	

The fact observed in the earlier three equation plot is also present here. Here the fitting is good but the first curve consists of almost 99.9% of the total drying curve.
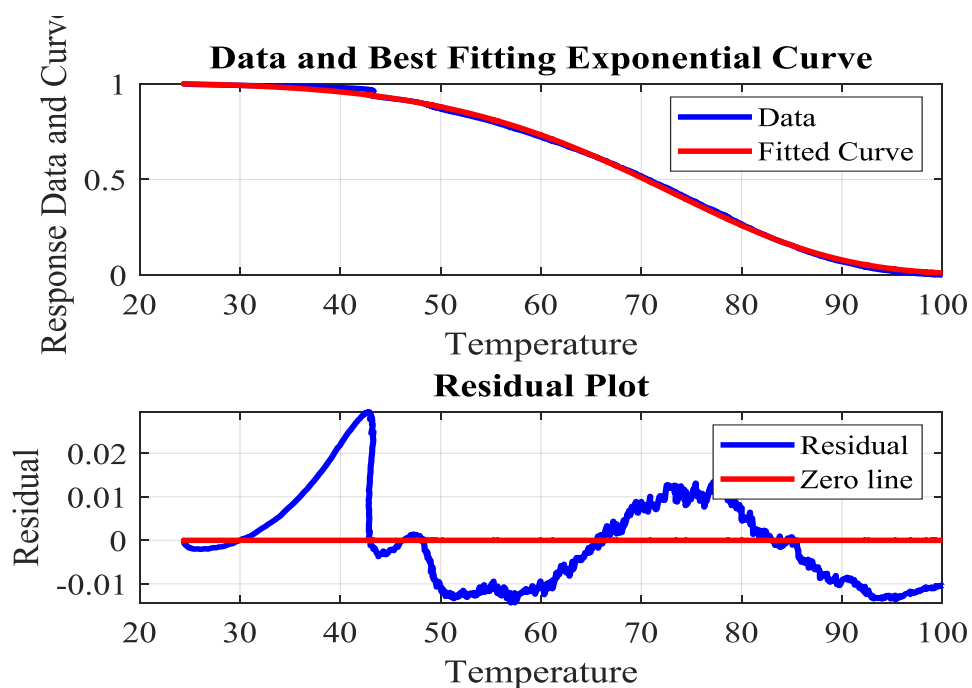
Figure 4-20: Curve fit for two curve fit

So, it can be concluded that there present three different kinds of moisture. But, for drying of microalgae only single type of moisture (Free water) removal is the key fact.

5. CONCLUSIONS AND RECOMMENDATIONS

5.1 Conclusion

Non-isothermal drying kinetics of *Chlorella vulgaris* species was studied using TGA at 5 K/min and 20 K/min heating rates. This algae species was chosen specially for this purpose as it is very high in lipid content, can be easily cultured and up-scaled and display the best suitability toward large scale oil production.

The algae sample was characterized. The mass loss as a function of temperature was recorded and the data was fitted using four kinetic models: Newton, Henderson and Pabis, Logarithmic, and Page models. The findings of the study are summarized below.

- Proximate analysis (wet basis) showed a significant amount of volatile content (>70%) presents in the sample. The ash content of the sample was found to be approximately 15%.

- Ultimate analysis reveals that Chlorella contains the higher heating value of about 12.63 MJ/Kg which is a significant amount.

- From the TGA and DTG data it is also clear that the water loss peaks take place at around 75°C-80°C. So, this temperature can be used as the most suitable drying temperature for bio-fuel production. Further studies are required to determine the nutraceutical value at different drying temperature.

- All four models show satisfactory result among which Page's model shows the best fit in both heating rate (5 K/min and 20 K/min) process. Page's model can be used in further studies to represent the drying kinetics of *Chlorella vulgaris*. Activation energy ranges from $49-53$ kJ.mol^{-1} for 5 K/min heating rate. The value decreases as the drying rate increase as observed for 20 K/min heating rate （$18-20$ kJ.mol^{-1}）.

- Presence of different types of moisture were also observed from DSC curve. It has been found that there exist three different kinds of moisture in the sample of microalgae. But, for drying of microalgae only single type of moisture (Free water) removal is the key fact. So, single equation fitting is quite good enough to represent the total drying process as there is only one type of water (free water) is significant to the process.

5.2 Future Recommendations

Based on findings from this study, the following measures can be proposed for extending the present work.

- There exists a number of microalgae species available which can also be tested in a comparative manner. This could reveal the actual viability of *Chlorella vulgaris*.

- Also, there are various strain of a microalgae. Testing of different varieties of *Chlorella vulgaris* strain can be done to make the study enriched.

- In this study, for curve fitting the data obtained from single heating rate has been used. But it would give much more accurate results if both heating rates data could have been considered simultaneously. This could be an important step to add for further research.

- Effect of moisture content over drying kinetics can also be observed for further studies. This would add new dimension to the research.

- Drying kinetics obtained from isothermal can be compared with the non-isothermal drying kinetics for comparative study. In literature, isothermal drying has been used for a number of agricultural products drying. So, it will help to make a comparison and enrich the research.

REFERENCES

[1] Lawton RJ, Cole AJ, Roberts DA, Paul NA, de Nys RJAR. The industrial ecology of freshwater macroalgae for biomass applications. Algal Research 2017;24:486-91.

[2] Klinthong W, Yang Y-H, Huang C-H, Tan C-SJAAQR. A review: microalgae and their applications in CO2 capture and renewable energy. Aerosol and Air Quality Research 2015;15(2):712-42.

[3] Powell E, Hill GJCER, Design. Economic assessment of an integrated bioethanol–biodiesel–microbial fuel cell facility utilizing yeast and photosynthetic algae. Chemical Engineering Research and Design 2009;87(9):1340-8.

[4] Demirbas A, Demirbas MFJEc, management. Importance of algae oil as a source of biodiesel. Energy Conversion and Management 2011;52(1):163-70.

[5] Hosseinizand H, Sokhansanj S, Lim CJJDT. Studying the drying mechanism of microalgae Chlorella vulgaris and the optimum drying temperature to preserve quality characteristics. Drying Technology 2018;36(9):1049-60.

[6] Villagracia AR, Mayol AP, Ubando A, Biona JBM, Arboleda Jr N, David M, et al. Microwave drying characteristics of microalgae (Chlorella vulgaris) for bio-fuel production. 2016.

[7] Salehi F, Kashaninejad M. Modeling of moisture loss kinetics and color changes in the surface of lemon slice during the combined infrared-vacuum drying. Information Processing in Agriculture 2018;5(4):516-23.

[8] Chen D, Zhang Y, Zhu XJE, Fuels. Drying kinetics of rice straw under isothermal and nonisothermal conditions: a comparative study by thermogravimetric analysis. Energy & Fuels 2012;26(7):4189-94.

[9] Vega- Gálvez A, Puente- Díaz L, Lemus- Mondaca R, Miranda M, Torres MJJJoFP, Preservation. Mathematical Modeling of Thin- Layer Drying Kinetics

of C ape Gooseberry (P hysalis peruviana L.). Journal of Food Processing and Preservation 2014;38(2):728-36.

[10]   Lewis WK. The Rate of Drying of Solid Materials. Journal of Industrial & Engineering Chemistry 1921;13(5):427-32.

[11]   Page GE. FACTORS INFLUENCING THE MAXIMUM RATES OF AIR DRYING SHELLED CORN IN THIN LAYERS. *Mechanical Engineering.* Master of Science USA: Purdue University; 1949.

[12]   Chandra P, Singh R. Applied Numerical Methods for Food and Agricultural Engineers. 2017.

[13]   Midilli A, Kucuk H, Yapar Z. A NEW MODEL FOR SINGLE-LAYER DRYING. Drying Technology 2002;20(7):1503-13.

[14]   Masojídek J, Torzillo G. Mass Cultivation of Freshwater Microalgae. 2008, p. 2226-35.

[15]   Brennan L, Owende PJR, reviews se. Bio-fuels from microalgae—a review of technologies for production, processing, and extractions of bio-fuels and co-products. Renewable and Sustainable Energy Reviews 2010;14(2):557-77.

[16]   Okoronkwo M, Galadima A, Luter L. Advances in Biodiesel synthesis: from past to present. 2012.

[17]   Becker EW. Microalgae: biotechnology and microbiology. Cambridge University Press; 1994.

[18]   Hajati H, Zaghari M. Spirulina Platensis in Poultry Nutrition. 2019.

[19]   Safi C, Zebib B, Merah O, Pontalier P-Y, Vaca-Garcia CJR, Reviews SE. Morphology, composition, production, processing and applications of Chlorella vulgaris: a review. Renewable and Sustainable Energy Reviews 2014;35:265-78.

[20]   Maruyama I, Nakao T, Shigeno I, Ando Y, Hirayama K. Application of unicellular algae Chlorella vulgaris for the mass-culture of marine rotifer Brachionus. Dordrecht: Springer Netherlands; 1997:133-8.

[21]   Varzakas T, Tzia C. Food Engineering Handbook, Two Volume Set. CRC Press; 2014.

[22]   Inyang U, Oboh I, Etuk B. Kinetic Models for Drying Techniques—Food Materials. Advances in Chemical Engineering and Science 2018;08:27-48.

[23]   Ahmed D-N, * J, Singh H, Chauhan P, Gupta A, Anjum H, et al. Different Drying Methods: Their Applications and Recent Advances. 2013.

[24]   Chen C-L, Chang J-S, Lee D-J. Dewatering and Drying Methods for Microalgae. Drying Technology 2015;33(4):443-54.

[25]   Hendorson SJJoAER. Grain Drying Theory (I) Temperature Effect on Drying Coefficient. Journal of Agricultural Engineering Research 1961;6(3):169-74.

[26]   Hawlader MNA, Uddin MS, Ho JC, Teng ABW. Drying characteristics of tomatoes. 1991.

[27]   Parti M. A theoretical model for thin layer grain drying. 1990.

[28]   Özdemir M, Devres Y. Turkish hazelnuts: Properties and effect of microbiological and chemical changes on quality. 1999.

[29]   D. B. Brooker FWB-AuCWH. Drying Cereal Grains. Westport: The Avi Publishing Company, Inc.; 1982.

[30]   Luikov AV. Heat and Mass Transfer in Capillary-Porous Bodies. In: Irvine TF, Hartnett JP, editors. Advances in Heat Transfer. Elsevier; 1964, p. 123-84.

[31]   Ekechukwu V, Norton B. Review of solar-energy drying systems III: Low temperature air-heating solar collectors for crop drying applications. 1999.

[32]   Crank J. The mathematics of diffusion. Oxford university press; 1979.

[33]   Overhults D, White G, Hamilton H, Ross IJJTotA. Drying Soybeans With Heated Air. Transactions of American Society of Agricultural Engineers 1973;16:112-0113.

[34] M. White G, C. Bridges T, J. Loewer O, J. Ross I. Seed Coat Damage in Thin-Layer Drying of Soybeans. Transactions of the ASAE 1980;23(1):224-0227.

[35] Diamante LM, Munro PA. Mathematical modelling of the thin layer solar drying of sweet potato slices. Solar Energy 1993;51(4):271-6.

[36] Zogzas NP, Maroulis ZB, Marinos-Kouris D. MOISTURE DEFFUSIVITY METHODS OF EXPERIMENTAL DETERMINATION AREVIEW. Drying Technology 1994;12(3):483-515.

[37] Madamba PS, Driscoll RH, Buckle KAJJofe. The thin-layer drying characteristics of garlic slices. Journal of Food Engineering 1996;29(1):75-97.

[38] Vega-Galvez A, Uribe E, Lemus-Mondaca R, Miranda M. Hot-air drying characteristics of Aloe vera (Aloe barbadensis Miller) and influence of temperature on kinetic parameters. 2007.

[39] L. Thompson T, Peart M, G. H. Foster R. Mathematical Simulation of Corn Drying — A New Model. Transactions of the ASAE 1968;11(4):582-0586.

[40] R. Paulsen M, L. Thompson T. Drying Analysis of Grain Sorghum. Transactions of the ASAE 1973;16(3):537-0540.

[41] Wang Z, Sun J, Chen F, Liao X, Hu X. Mathematical modeling on thin layer microwave drying of apple pomace with and without hot-air pre drying. Journal of Food Engineering 2007;80:536-44.

[42] Shaik K, Kailappan R. Modelling of thin-layer drying kinetics of red chillies. Journal of Food Engineering 2006;76:531-7.

[43] Benemann J, Goebel R, Weissman J, Augenstein D. Microalgae as a source of liquid fuels. *Proceedings of the June 1982 SERI Biomass Program Principal Investigators' Review Meeting, Aquatic Species Program Reports.* 1982:1-16.

[44] Benemann JR, Weissman JC, Koopman BL, Oswald WJJN. Energy production by microbial photosynthesis. Nature 1977;268(5615):19.

[45]   Kiranoudis CT, Tsami E, Maroulis ZB, Marinos-Kouris D. DRYING KINETICS OF SOME FRUITS. Drying Technology 1997;15(5):1399-418.

[46]   Deng X, Gao K, Addy M, Chen P, Li D, Zhang R, et al. Growing Chlorella vulgaris on mixed wastewaters for biodiesel feedstock production and nutrient removal. Chemical Technology and Biotechnology 2018;93(9):2748-57.

APPENDIX

Microalgae Culture

Figure 1: Production facilities of microalgae used for this work

Figure 2: A glimpse of testing at BCSIR; BUET Chemical Engineering Laboratory and CARS, DU.

Proximate Analysis

Sample: *Chlorella vulgaris*

Condition: Dried at 75 °C for 3 hours

Results Summary:

Proximate Analysis (Wt%)

Moisture Content	6.67 %
Volatile	70.51 %
Ash Content	15.46 %
Fixed Carbon	7.36 %

Heating Value

Higher Heating Value	12.63 MJ/Kg

Water Content/ Moisture Content

Name of the parameter: Water Content/ Moisture Content

Sample: *Chlorella vulgaris* dried at 75 °C for 3 hours

Experiment Method: ASTM D 95

Experimental Data:

Weight of Empty Petri Dish (w_d)	58.372 gm
Weight of Petri Dish with Sample (w_1)	59.376 gm
Weight of Sample: (w_s)	1.004 gm
After drying at 105 °C for 1 hour	
Weight of Petri Dish with Sample (w_2)	59.309 gm
Moisture/ Water Content, w = (w_1-w_2)	0.067 gm

So, The Moisture Content of the sample is $= \dfrac{w \times 100}{w_s}$

$$= \dfrac{0.067 \times 100}{1.004}$$

$$= 6.67\%$$

Result:

Moisture / Water Content	6.67 % (Wet Basis)

Volatile

Name of the parameter: Volatile

Sample: *Chlorella vulgaris* dried at 75 °C for 3 hours

Experiment Method: ASTM D 5142

Experimental Data:

Weight of Empty Crucible (w_d)	14.158 gm
Weight of Crucible with Sample (w_1)	15.155 gm
Weight of Sample: ($w = w_1 - w_d$)	00.997 gm
After 7 minutes in oven at 900 °C	
Weight of Crucible with Sample (w_2)	14.452 gm
Volatile Content, V = ($w_1 - w_2$)	00.703 gm

Volatile Content of the Sample $\quad = \dfrac{V \times 100}{w}$

$$= \frac{0.703 \times 100}{0.997}$$

$$= 70.51\ \%$$

Result:

Volatile	70.51%

Ash Content

Name of the parameter: Ash Content

Sample: *Chlorella vulgaris* dried at 75 °C for 3 hours

Experiment Method: ASTM D 5142

Experimental Data:

Weight of Empty Crucible (w_d)	34.094 gm
Weight of Crucible with Sample (w_1)	35.019 gm
Weight of Sample: ($w = w_1 - w_d$)	00.925 gm
After 20 minutes in oven at 700 °C	
Weight of Crucible with Sample (w_2)	34.237 gm
Final Weight of Sample (Ash), A = ($w_2 - w_d$)	00.143 gm

Ash Content of the Sample $= \dfrac{A \times 100}{w}$

$$= \dfrac{0.143 \times 100}{0.925}$$

$$= 15.46 \%$$

Result:

Ash Content	15.46 %

Fixed Carbon

Name of the parameter: Fixed Carbon

Sample: *Chlorella vulgaris* dried at 75 °C for 3 hours

Experiment Method: ASTM D 5142

Experimental Data:

From Previous Experiment,

Moisture Content	6.67 %
Volatile	70.51 %
Ash Content	15.46%

Fixed carbon of the Sample   =100- (Moisture Content+ Volatile+ Ash Content)

= [100-(6.67+70.51+15.46)] %

= 7.36%

Result:

Fixed Carbon	7.36 %

Calorific Value

Name of the parameter: Calorific Value

Sample: *Chlorella vulgaris* dried at 75 °C for 3 hours

Experiment Method: ASTM D 2015

Experimental Data:

Weight of Sample Taken in Crucible (m)	0.9942 gm
Initial Temperature (T_i)	87.5 °F = 30.83 °C
Final Temperature (T_i)	89.7 °F = 32.07 °C
Rise in Water Temperature ($\Delta T = T_f - T_i$)	1.23 °C

O2 Pressure in Bomb = 25 bar

Calorific Value, $C_v = \dfrac{[(mCp)b + (mCp)w\,]\Delta T - (mu)_c}{m}$

Where,

Energy equivalent factor of the calorimeter $(mCp)_b + (mCp)_w$ = 2463 cal/°C

Correction for fused copper wire and others $(mu)_c$ = 30 cal

So, Calorific Value C_v $= \dfrac{(2463 \times 1.23) - 30}{0.9942}$ cal/g

$= \dfrac{2999.49}{0.9942}$ cal/g

= 3017 kCal/Kg

= 12.63 MJ/Kg

Result:

Calorific Value (HHV)	12.63 MJ/Kg

Matlab codes for fitting:

```matlab
%------------Defining random number type------------%
rng default % for reproducibility

%------------Data Read from Excel File------------%
xData = xlsread('Data.xlsx','A2:A834')';
yData = xlsread('Data.xlsx','C2:C834')';

%------------Defining Function (from bottom)------------%
fun = @(x)rmseval(x,xData,yData);
gs = GlobalSearch;

%------------Defining Initial points------------%

%<<<<<<<<<======Choose any one======>>>>>>>>>
% x0 = rand(1,2); %Newton
% x0 = rand(1,3); %Henderson and Pabis
% x0 = rand(1,4); %Logarithmic
x0 = rand(1,3); %Page

%------------Performing best fit------------%
%<<<<<<<<<<<<<<<<  FORMAT  >>>>>>>>>>>>>>>>>>>>>%
    %FMINCON(FUN,X0,A,B,Aeq,Beq,LB,UB,NONLCON,OPTIONS)

%        createOptimProblem('fmincon','objective', FUN, 'x0', X0, ...
%        'Aineq', A, 'bineq', b, 'Aeq', Aeq, 'beq', beq, 'lb', LB, ...
%        'ub', UB, 'nonlcon', NONLCON, 'options', OPTIONS)

%<<<<<<<<<<<<<<<<<<<<<<< ====== Choose any one ======
>>>>>>>>>>>>>>>>>>>>
% bestx = createOptimProblem('fmincon','objective',fun,'x0',x0,...
%  'Aineq',[-1 0;0 -1],'bineq',[0;0]); %Newton

% bestx = createOptimProblem('fmincon','objective',fun,'x0',x0,...
%  'Aineq',[-1 0 0;0 -1 0;0 0 -1],'bineq',[0;0;0]); %Henderson

% bestx = createOptimProblem('fmincon','objective',fun,'x0',x0,...
%  'Aineq',[-1 0 0 0;0 -1 0 0;0 0 -1 0; 0 0 0 -1],'bineq',[0;0;0;0]); %Logarithmic

bestx = createOptimProblem('fmincon','objective',fun,'x0',x0,...
'Aineq',[-1 0 0;0 -1 0;0 0 -1],'bineq',[0;0;0]); %Page


Globalx = run(gs,bestx);

%<<<<<<<<<<<<<<<<<<<<<<< ====== Choose any one ======
>>>>>>>>>>>>>>>>>>>>
% E = Globalx(1);k = Globalx(2); %Newton
% a = Globalx(1);E = Globalx(2);k = Globalx(3); %Henderson
% a = Globalx(1);c = Globalx(2);E = Globalx(3);k = Globalx(4); %Logarithmic
```

```matlab
E = Globalx(1);k = Globalx(2);n = Globalx(3); %Page



%------------Plot Graph and compare with experimental value------------%

%<<<<<<<<<<<<<<<<<<<<<<< ======= Choose any one  =======
>>>>>>>>>>>>>>>>>>>
% Curve=(exp(-k.*exp((-E./(0.008314.*(xData+273.15)))).*((xData-24.441)./5)));
%Newton
% Curve=a.*(exp(-k.*exp((-E./(0.008314.*(xData+273.15)))).*((xData-24.441)./5)));
%Henderson
% Curve=a.*(exp(-k.*exp((-E./(0.008314.*(xData+273.15)))).*((xData-24.441)./5)))+c;
%Logarithmic
Curve=(exp(-k.*exp((-E./(0.008314.*(xData+273.15)))).*(((xData-24.4)./5).^n)));
%Logarithmic

yfit=Curve;
Res=yData-yfit;
Zero=0.*xData;

subplot( 2, 1, 1 );
plot(xData,yData,'b','LineWidth',2.5);
hold on
plot(xData,yfit,'r','LineWidth',2.5);
xlabel('Temperature')

ylabel('MR')

title('Data and Best Fitting Exponential Curve')
legend('Data','Fitted Curve (Page)','Location','southwest')
grid on
hold off;
set(gca,'FontSize',14,'FontName','Times New Roman');
% Plot residuals.
subplot( 2, 1, 2 );
plot(xData,Res,'b','LineWidth',2.5);
hold on
plot(xData,Zero,'r','LineWidth',2.5);
xlabel('Temperature')
ylabel('Residual')
title('Residual Plot')
legend('Residual','Zero line')
grid on
hold off;
set(gca,'FontSize',14,'FontName','Times New Roman');
%----------R2 value----------%
yresid = yData - yfit;
SSresid = sum(yresid.^2);
SStotal = (length(yData)-1) * var(yData);
```

```matlab
rsq = 1 - SSresid/SStotal;
rsq_adj = 1 - SSresid/SStotal * (length(yData)-1)/(length(yData)-length(x0));
RMSE = sqrt(mean((yData - yfit).^2));
Chi2=sum((yData - yfit).^2)/(length(xData)-length(x0));


%------------Showing Results------------%
% fprintf('E= %d\n', Globalx(1));fprintf('k= %d\n', Globalx(2));% Newton
% fprintf('a= %d\n', Globalx(1));fprintf('E= %d\n', Globalx(2));fprintf('k= %d\n',
Globalx(3));% Henderson
% fprintf('a= %d\n', Globalx(1));fprintf('c= %d\n', Globalx(2));fprintf('E= %d\n',
Globalx(3));fprintf('k= %d\n', Globalx(4));% Logarithm
fprintf('E= %d\n', Globalx(1));fprintf('k= %d\n', Globalx(2));fprintf('n= %d\n',
Globalx(3));% Page

fprintf('rsq= %d\n',rsq);
fprintf('rsq_adj= %d\n',rsq_adj);fprintf('Chi2= %d\n', Chi2);
fprintf('RMSE= %d\n', RMSE);



%------------MAIN FUNCTION------------%
function RMSE = rmseval(x,xData,yData)
%<<<<<<<<<<<<<<<<<<<<<< ======= Choose any one =======
>>>>>>>>>>>>>>>>>>>>>
% E = x(1);k = x(2);%Newton
% a = x(1);E = x(2);k=x(3);%Henderson
% a = x(1);c = x(2);E=x(3);k=x(4);%Logarithmic
E = x(1);k = x(2);n=x(3);%Page

% Curve=(exp(-k.*exp((-E./(0.008314.*(xData+273.15)))).*((xData-24.441)./5)));
%Newton
% Curve=a.*(exp(-k.*exp((-E./(0.008314.*(xData+273.15)))).*((xData-24.441)./5)));
%Henderson
% Curve=a.*(exp(-k.*exp((-E./(0.008314.*(xData+273.15)))).*((xData-24.441)./5)))+c;
%Logarithmic
Curve=(exp(-k.*exp((-E./(0.008314.*(xData+273.15)))).*(((xData-24.4)./5).^n)));
%Page
yCalc=Curve;
RMSE = sqrt(mean((yData - yCalc).^2));
end
```